

QCD Running in Lepton Number Violating Meson and Tau Decays

Marcela González^{1*}; Nicolás A. Neill^{2†}

¹*Instituto de Física y Astronomía, Universidad de Valparaíso,
Avenida Gran Bretaña 1111, Valparaíso, Chile*

²*Universidad de Tarapacá, Departamento de Ingeniería Eléctrica-Electrónica,
Arica, Chile*

Abstract

Below the electroweak scale, new physics that violates lepton number in two units ($\Delta L = 2$) and is mediated by heavy particle exchange can be parameterized by a dimension-9 low-energy effective Lagrangian. Operators in this Lagrangian involving first-generation quarks and leptons contribute to the short-range mechanism of neutrinoless double beta decay ($0\nu\beta\beta$) and therefore they are strongly constrained. On the other hand, operators with other quark and lepton families are bounded by the non-observation of different lepton number violating (LNV) meson and tau decays, such as $M_1^- \rightarrow M_2^+ \ell_1^- \ell_2^-$ and $\tau^- \rightarrow \ell^+ M_1^- M_2^-$. In this work, we calculate RGE-improved bounds on the Wilson coefficients involved in these decays. We calculate QCD corrections to the dimension-9 operator basis and find RG evolution matrices that describe the evolution of the Wilson coefficients across different energy scales. Unlike the running of operators involved in $0\nu\beta\beta$ -decay, the general flavor structure leads to the mixing of not only different Lorentz structures but also of different quark-flavor configurations. Additionally, operators that vanish for the identical lepton case need to be added to the operator basis. We find new constraints on previously unbounded operators and the enhancement of bounds for specific Wilson coefficients. We also find new bounds coming from the mixing between operators with different quark-flavor configurations.

*marcela.gonzalezpi@uv.cl

†naneill@outlook.com

1 Introduction

The origin of neutrino masses and mixing remains an open question that requires physics beyond the standard model. If neutrinos are Dirac fermions, the physics responsible for neutrino masses conserves total lepton number (L). On the other hand, it is known that the existence of new physics that violates lepton number in two units ($\Delta L = 2$) would imply the generation of Majorana mass terms at the loop level [1]. Therefore, the observation of a lepton number violating (LNV) process would shed light on the type of new physics responsible for neutrino masses and on the Dirac vs. Majorana nature of neutrinos.

Many experiments have searched for LNV in different processes. The golden channel for the observation of LNV is neutrinoless double beta ($0\nu\beta\beta$) decay [2, 3], which puts stringent bounds on the $0\nu\beta\beta$ -decay half-life ($T_{1/2} \gtrsim 2.3 \times 10^{26}$ yr [4]). Other processes that are sensitive to lepton-number violation include meson decays such as $K^- \rightarrow \pi^+ \mu^- \mu^-$ [5–27], tau-lepton decays such as $\tau^- \rightarrow e^+ \pi^- \pi^-$ [28–32], $\ell_1^- \rightarrow \ell_2^+$ lepton conversion [33–37], and collider searches with same-sign leptons in the final state [38–42]. Unlike $0\nu\beta\beta$ -decay, both meson and tau decays allow to prove LNV interactions that are not restricted to first generation quarks and leptons.

The new LNV physics can be described in a model-independent way by using low energy effective Lagrangians. In particular, dimension-9 operators involving first-generation quarks and leptons have been used to parameterize the different contributions to $0\nu\beta\beta$ -decay mediated by heavy particle exchange (the so-called short-range mechanism) [43], allowing to find model-independent bounds on the corresponding Wilson coefficients. Meson and tau decays have also been used to put tree-level constraints on dimension-9 LNV operators involving quarks and leptons not restricted to the first generation [44]. The effects of renormalization group evolution (RGE) have proven to be relevant when extracting bounds on the Wilson coefficients contributing to $0\nu\beta\beta$ -decay [41, 45–50], as well as putting bounds on new physics in other contexts, such as flavor physics [51], meson and tau decays [52–55], and dark matter direct detection [56, 57].

In this work, we derive the renormalization group evolution for the complete dimension-9 LNV ($\Delta L = 2$) operator basis contributing to the LNV meson and tau decays, $M_1^- \rightarrow M_2^+ \ell_1^- \ell_2^-$ and $\tau^- \rightarrow \ell^+ M_1^- M_2^-$, respectively.¹ This basis, with operators of the form $\mathcal{O} \sim (\bar{u}_i \Gamma_1 d_j)(\bar{u}_k \Gamma_2 d_l)(\bar{\ell}_1 \Gamma_3 \ell_2^c)$, is a generalization of the basis considered in the short-range mechanism of $0\nu\beta\beta$ -decay since it is not constrained to first-generation quarks, and in general $\ell_1 \neq \ell_2$. As we will show in Sec. (3), this introduces additional operators (not present for equal lepton flavors) and additional quark mixings. We apply this results to extract RGE-improved bounds on the Wilson coefficients relevant to the meson and tau decays listed in Tables (1) and (2).²

Our paper is organized as follows. In Section (2) we present the dimension-9 low energy effective Lagrangian and review how tree-level bounds on Wilson coefficients are derived from

¹The conjugate processes are implied here and throughout the text.

²Present and upcoming experiments are expected improve these bounds [25]. For instance, the High Intensity Kaon Experiments (HIKE) [58] are expected to probe the branching fraction of $K^- \rightarrow \pi^+ \ell^- \ell^-$ with a sensitivity of $\mathcal{O}(10^{-13})$, while current constraints on D - and B -meson decays from LHCb, based on integrated luminosities of $\mathcal{O}(1 \text{ fb}^{-1})$, could improve by approximately two orders of magnitude as the target luminosity (300 fb^{-1}) is achieved. Similarly, current bounds derived from BaBar and Belle experiments could be improved by up to two orders of magnitude once the target luminosity of Belle-II (50 ab^{-1}) is reached.

LNV meson and tau decays. In Section (3) we calculate QCD corrections to the dimension-9 LNV basis and find the anomalous dimension and evolution matrices. These results are applied in Section (4) to find new RGE-induced bounds on the Wilson coefficients, which are the main result of our work together with the anomalous dimensions for the general case with arbitrary quark and lepton flavors. Finally, our summary and conclusions are presented in Section (5).

2 LNV Effective Lagrangian and LNV Decays

The most general low energy dimension-9 effective Lagrangian that involves quark currents and violates lepton number in two units ($\Delta L = 2$) can be written as

$$\mathcal{L}_{\text{eff}}^{\Delta L=2} = \frac{G_F^2}{2m} \sum_{\substack{n,XYZ \\ ijkl,\ell_1\ell_2}} C_{n(ijkl)}^{XYZ(\ell_1\ell_2)}(\mu) \cdot \mathcal{O}_{n(ijkl)}^{XYZ(\ell_1\ell_2)}(\mu), \quad (1)$$

where m is a mass scale that we will choose depending of the process in consideration, $C_{n(ijkl)}^{XYZ(\ell_1\ell_2)}$ are Wilson coefficients, and $\mathcal{O}_{n(ijkl)}^{XYZ(\ell_1\ell_2)}$ are a complete basis for the LNV ($\Delta L = 2$) dimension-9 operators:

$$\mathcal{O}_{1(ijkl)}^{XYZ(\ell_1\ell_2)} = 8(\bar{u}_i P_X d_j)(\bar{u}_k P_Y d_l) j^Z, \quad (2)$$

$$\mathcal{O}_{2(ijkl)}^{XXX(\ell_1\ell_2)} = 8(\bar{u}_i \sigma^{\mu\nu} P_X d_j)(\bar{u}_k \sigma_{\mu\nu} P_X d_l) j^X, \quad (3)$$

$$\mathcal{O}_{3(ijkl)}^{XYZ(\ell_1\ell_2)} = 8(\bar{u}_i \gamma^\mu P_X d_j)(\bar{u}_k \gamma_\mu P_Y d_l) j^Z, \quad (4)$$

$$\mathcal{O}_{4(ijkl)}^{XYZ(\ell_1\ell_2)} = 8(\bar{u}_i \gamma^\mu P_X d_j)(\bar{u}_k \sigma_\mu^\nu P_Y d_l) j_\nu^Z, \quad (5)$$

$$\mathcal{O}_{5(ijkl)}^{XYZ(\ell_1\ell_2)} = 8(\bar{u}_i \gamma^\mu P_X d_j)(\bar{u}_k P_Y d_l) j_\mu^Z. \quad (6)$$

$$\mathcal{O}_{6(ijkl)}^{XYZ(\ell_1\ell_2)} = 8(\bar{u}_i \gamma^\mu P_X d_j)(\bar{u}_k \gamma^\nu P_Y d_l) j_{\mu\nu}^Z, \quad (7)$$

$$\mathcal{O}_{7(ijkl)}^{XZZ(\ell_1\ell_2)} = 8(\bar{u}_i P_X d_j)(\bar{u}_k \sigma^{\mu\nu} P_Z d_l) j_{\mu\nu}^Z, \quad (8)$$

$$\mathcal{O}_{8(ijkl)}^{XXX(\ell_1\ell_2)} = 8(\bar{u}_i \sigma^{\mu\alpha} P_X d_j)(\bar{u}_k \sigma_\alpha^\nu P_X d_l) j_{\mu\nu}^X, \quad (9)$$

with

$$j^Z = \bar{\ell}_1 P_Z \ell_2^c, \quad j_\mu^Z = \bar{\ell}_1 \gamma^\mu P_Z \ell_2^c, \quad j_{\mu\nu}^Z = \bar{\ell}_1 \sigma^{\mu\nu} P_Z \ell_2^c, \quad (10)$$

Process	Limit on BR	Process	Limit on BR	Process	Limit on BR
$K^- \rightarrow \pi^+ e^- e^-$	5.3×10^{-11} [5]	$K^- \rightarrow \pi^+ \mu^- \mu^-$	4.2×10^{-11} [6]	$K^- \rightarrow \pi^+ e^- \mu^-$	4.2×10^{-11} [7]
$D^- \rightarrow \pi^+ e^- e^-$	5.3×10^{-7} [8]	$D^- \rightarrow \pi^+ \mu^- \mu^-$	1.4×10^{-8} [8]	$D^- \rightarrow \pi^+ e^- \mu^-$	1.3×10^{-7} [8]
$D^- \rightarrow K^+ e^- e^-$	9.0×10^{-7} [9]	$D^- \rightarrow K^+ \mu^- \mu^-$	1.0×10^{-5} [9]	$D^- \rightarrow K^+ e^- \mu^-$	1.9×10^{-6} [9]
$D_s^- \rightarrow \pi^+ e^- e^-$	1.4×10^{-6} [8]	$D_s^- \rightarrow \pi^+ \mu^- \mu^-$	8.6×10^{-8} [8]	$D_s^- \rightarrow \pi^+ e^- \mu^-$	6.3×10^{-7} [8]
$D_s^- \rightarrow K^+ e^- e^-$	7.7×10^{-7} [8]	$D_s^- \rightarrow K^+ \mu^- \mu^-$	2.6×10^{-8} [8]	$D_s^- \rightarrow K^+ e^- \mu^-$	2.6×10^{-7} [8]
$B^- \rightarrow \pi^+ e^- e^-$	2.3×10^{-8} [10]	$B^- \rightarrow \pi^+ \mu^- \mu^-$	4.0×10^{-9} [11]	$B^- \rightarrow \pi^+ e^- \mu^-$	1.5×10^{-7} [12]
$B^- \rightarrow K^+ e^- e^-$	3.0×10^{-8} [10]	$B^- \rightarrow K^+ \mu^- \mu^-$	4.1×10^{-8} [13]	$B^- \rightarrow K^+ e^- \mu^-$	1.6×10^{-7} [12]
$B^- \rightarrow D^+ e^- e^-$	2.6×10^{-6} [12, 14]	$B^- \rightarrow D^+ \mu^- \mu^-$	6.9×10^{-7} [15]	$B^- \rightarrow D^+ e^- \mu^-$	1.8×10^{-6} [14]
		$B^- \rightarrow D_s^+ \mu^- \mu^-$	5.8×10^{-7} [15]		

Table 1: Current experimental upper bounds on the branching ratios (BR) of different LNV meson decays.

Process	Limit on BR [28]	Process	Limit on BR [28]
$\tau^- \rightarrow e^+ \pi^- \pi^-$	2.0×10^{-8}	$\tau^- \rightarrow \mu^+ \pi^- \pi^-$	3.9×10^{-8}
$\tau^- \rightarrow e^+ \pi^- K^-$	3.2×10^{-8}	$\tau^- \rightarrow \mu^+ \pi^- K^-$	4.8×10^{-8}
$\tau^- \rightarrow e^+ K^- K^-$	3.3×10^{-8}	$\tau^- \rightarrow \mu^+ K^- K^-$	4.7×10^{-8}

Table 2: Current experimental upper bounds on the branching ratios (BR) of different LNV tau decays.

where P_X are chiral projectors with the indices $X, Y, Z = L, R$ the corresponding chiralities, while the indices $i, j = u, c$ and $k, l = d, s, b$ run over the quark flavors and $\ell_1, \ell_2 = e, \mu, \tau$ over lepton flavors. The factor eight in front of the definition of the operators has been introduced for consistency with the basis without chiral projectors [43]. Operators $\mathcal{O}_2, \mathcal{O}_7$, and \mathcal{O}_8 appear with repeated chiralities since $\sigma^{\mu\nu} P_X \otimes \sigma_{\mu\nu} P_Y = 0$ for $X \neq Y$ and $\sigma^{\mu\alpha} P_X \otimes \sigma'_\alpha P_Y \otimes \sigma_{\mu\nu} P_Z$ is non vanishing only for $X = Y = Z$, as can be shown by Fierz transformations. Additionally, for $\ell_1 = \ell_2$, the operators $\mathcal{O}_{6,7,8}$ vanish since $\bar{\ell} \sigma^{\mu\nu} P_X \ell^c \equiv 0$. In this work, we consider meson decays with both same and different flavor leptons in the final state, and tau lepton decays that, due to kinematics, necessarily involve different lepton flavors. Therefore, we will consider the full basis (\mathcal{O}_n , with $n = 1, \dots, 8$) shown in Eqs. (2-9). For $\ell_1 = \ell_2 = e$, the subset of operators $\mathcal{O}_{1,2,3,4,5}$ involving first generation quarks (i.e., $ijkl = udud$) contribute to the short-range mechanism of $0\nu\beta\beta$ -decay, which has been already studied in the literature [43, 46, 59]. Given the strong bounds on the $0\nu\beta\beta$ -decay lifetime, the Wilson coefficients $\mathcal{O}_{1,2,3,4,5}^{XYZ(ee)}$ are strongly constrained (with bounds of the order $\sim \mathcal{O}(10^{-7}) \rightarrow \mathcal{O}(10^{-9})$ depending on the operator [43, 46]). On the other hand, Wilson coefficients with other quark flavors ($ijkl \neq udud$) or other lepton flavors ($\ell_1 \ell_2 \neq ee$) are not constrained by $0\nu\beta\beta$ -decay. These Wilson coefficients are constrained by the meson and tau decays considered in this work: the meson decays $M_1^- \rightarrow M_2^+ \ell_1^- \ell_2^-$ put bounds on operators with $ijkl \neq udud$ since they necessarily include at least one non-first-generation quark, while the tau decays $\tau^- \rightarrow \ell^+ M_1^- M_2^-$ constrain operators involving different lepton flavors ($\ell_1 \neq \ell_2$).

The tree-level amplitudes for the process $M_1^- \rightarrow M_2^+ \ell_1^- \ell_2^-$ mediated by the effective Lagrangian in Eq. (1) are given by

$$\mathcal{M}(M_1^- \rightarrow M_2^+ \ell_1^- \ell_2^-) = \langle M_2^+ \ell_1^- \ell_2^- | \mathcal{L}_{eff}^{\Delta L=2} | M_1^- \rangle = \frac{G_F^2}{2m_{M_1}} \sum_{\substack{n, XYZ \\ ijkl, \ell_1 \ell_2}} C_{n(ijkl)}^{XYZ(\ell_1 \ell_2)} \mathcal{A}_{n(ijkl)}^{XYZ(\ell_1 \ell_2)}, \quad (11)$$

where $\mathcal{A}_{n(ijkl)}^{XYZ(\ell_1 \ell_2)} = \langle M_2^+ \ell_1^- \ell_2^- | \mathcal{O}_{n(ijkl)}^{XYZ(\ell_1 \ell_2)} | M_1^- \rangle$ and $M_1^- = (\bar{u}_i d_j)$, $M_2^+ = (u_k \bar{d}_l)$. Parameterizing the hadronic matrix elements as

$$\langle 0 | \bar{u}_i \gamma^5 d_j | M \rangle = i \xi_M f_M, \quad \xi_M = \frac{m_M^2}{m_{u_i} + m_{d_j}}, \quad \langle 0 | \bar{u}_i \gamma^\mu \gamma^5 d_j | M \rangle = i p^\mu f_M, \quad (12)$$

where p^μ is the momentum of the meson M , we find:

$$\mathcal{A}_1^{XYZ} = \pm 2 f_{M_1} f_{M_2} \xi_{M_1} \xi_{M_2} [\bar{u}(p_{\ell_1}) P_Z v(p_{\ell_2})], \quad (13)$$

$$\mathcal{A}_3^{XYZ} = \pm 2 f_{M_1} f_{M_2} (p_M \cdot p'_M) [\bar{u}(p_{\ell_1}) P_Z v(p_{\ell_2})], \quad (14)$$

$$\mathcal{A}_5^{XYZ} = \pm 2 f_{M_1} f_{M_2} \xi_{M_2} p_M^\mu [\bar{u}(p_{\ell_1}) \gamma_\mu P_Z v(p_{\ell_2})], \quad (15)$$

$$\mathcal{A}_6^{XYZ} = \pm 2 f_{M_1} f_{M_2} p_{M_1}^\mu p_{M_2}^\nu [\bar{u}(p_{\ell_1}) \sigma_{\mu\nu} P_Z v(p_{\ell_2})], \quad (16)$$

where in the previous expressions the global + and - signs correspond to the cases $X = Y$ and $X \neq Y$, respectively. The amplitudes \mathcal{A}_2 , \mathcal{A}_4 , \mathcal{A}_7 , and \mathcal{A}_8 are not present since meson decay modes mediated by tensor currents are suppressed (vanish to first order) [44, 60].

The partial decay widths for the meson decays are given by [44]

$$\Gamma(M_1^- \rightarrow M_2^+ \ell_1^- \ell_2^-) = \left(1 - \frac{1}{2}\delta_{\ell_1 \ell_2}\right) \frac{G_F^4}{128(2\pi)^3 m_{M_1}^5} \times \sum_{n, XYZ} \left| C_{n(ijkl)}^{XYZ(\ell_1 \ell_2)} \right| \int_{s^-}^{s^+} ds \int_{t^-}^{t^+} dt \left| \overline{\mathcal{A}}_{n(ijkl)}^{XYZ(\ell_1 \ell_2)} \right|^2, \quad (17)$$

where $\overline{\mathcal{A}}_n$ are the spin-averaged amplitudes found in Eqs. (13)-(16), $s \equiv (p_{\ell_1} + p_{\ell_2})^2$, $t \equiv (p_{\ell_2} + p_{M_2})^2$, the integration limits are given by

$$s^- = (m_{\ell_1} + m_{\ell_2})^2, \quad s^+ = (m_{M_1} - m_{M_2})^2, \quad (18)$$

$$t^\pm = m_{M_1}^2 + m_{\ell_1}^2 - \frac{1}{2s} \left[(s + m_{M_1}^2 - m_{M_2}^2) \left(s + m_{M_{\ell_1}}^2 - m_{M_{\ell_2}}^2 \right) \mp \lambda^{1/2}(s, m_{\ell_1}^2, m_{\ell_2}^2) \lambda^{1/2}(s, m_{M_1}^2, m_{M_2}^2) \right], \quad (19)$$

with $\lambda(x, y, z) = x^2 + y^2 + z^2 - 2(xy + xz + yz)$, and the quark flavor indices (i, j, k, l) are fixed by the quark content of the mesons: $M_1^- = (\bar{u}_i d_j)$, $M_2^+ = (u_k \bar{d}_l)$.

Equivalently, for tau lepton decays, the tree-level amplitude for the process $\tau^- \rightarrow \ell^+ M_1^- M_2^-$ is given by

$$\mathcal{M}(\tau^- \rightarrow \ell^+ M_1^- M_2^-) = \langle \ell^+ M_1^- M_2^- | \mathcal{L}_{eff}^{\Delta L=2} | \tau^- \rangle = \frac{G_F^2}{2m_\tau} \sum_{n, XYZ} C_{n(ijkl)}^{XYZ(\tau \ell)} \mathcal{T}_{n(ijkl)}^{XYZ(\tau \ell)}, \quad (20)$$

where $\mathcal{T}_{n(ijkl)}^{XYZ(\tau \ell)} = \langle \ell^+ M_1^- M_2^- | \mathcal{O}_{n(ijkl)}^{XYZ(\tau \ell)} | \tau^- \rangle$ and $M_1^- = (\bar{u}_i d_j)$, $M_2^- = (\bar{u}_k d_l)$. Using the same parameterization for the hadronic matrix elements [Eq. (12)], we find similar expressions for \mathcal{T}_n as for \mathcal{A}_n in Eqs. (13)-(16), with the replacement $p_{\ell_1} \rightarrow p_\tau$ and $p_{\ell_2} \rightarrow p_\ell$. The partial decay widths for the tau lepton are given by [44]

$$\Gamma(\tau^- \rightarrow \ell^+ M_1^- M_2^-) = \left(1 - \frac{1}{2}\delta_{M_1 M_2}\right) \frac{G_F^4}{256(2\pi)^3 m_\tau^5} \times \sum_{n, XYZ} \left| C_{n(ijkl)}^{XYZ(\tau \ell)} \right| \int_{\tilde{s}^-}^{\tilde{s}^+} d\tilde{s} \int_{\tilde{t}^-}^{\tilde{t}^+} d\tilde{t} \left| \overline{\mathcal{T}}_{n(ijkl)}^{XYZ(\tau \ell)} \right|^2, \quad (21)$$

where $\overline{\mathcal{T}}_n$ are the spin-averaged amplitudes, $\tilde{s} \equiv (p_{M_1} + p_{M_2})^2$, $\tilde{t} \equiv (p_\ell + p_{M_2})^2$, the integration limits are given by

$$\tilde{s}^- = (m_{M_1} + m_{M_2})^2, \quad \tilde{s}^+ = (m_\tau - m_\ell)^2, \quad (22)$$

$$\tilde{t}^\pm = m_\tau^2 + m_{M_1}^2 - \frac{1}{2\tilde{s}} \left[(\tilde{s} + m_\tau^2 - m_\ell^2) \left(\tilde{s} + m_{M_{M_1}}^2 - m_{M_{M_2}}^2 \right) \mp \lambda^{1/2}(\tilde{s}, m_\tau^2, m_\ell^2) \lambda^{1/2}(\tilde{s}, m_{M_1}^2, m_{M_2}^2) \right], \quad (23)$$

where the quark flavor indices (i, j, k, l) are fixed by the quark content of the final mesons: $M_1^- = (\bar{u}_i d_j)$, $M_2^- = (\bar{u}_k d_l)$.

Eqs. (17) and (21) allow to find tree-level bounds on the Wilson coefficients $C_{n(ijkl)}^{XYZ(\ell_1 \ell_2)}$, which we will use in Sec. (4) to find RGE-improved bounds.

3 QCD running of WC for $|\Delta L| = 2$ Processes

In this section, we derive the QCD running of the WCs corresponding to the LNV ($\Delta L = 2$) effective operator basis presented in Ecs. (2)-(9), which contributes to the meson and tau decays discussed in the previous sections ($M_1^- \rightarrow M_2^+ \ell_1^- \ell_2^-$ and $\tau^- \rightarrow \ell^+ M_1^- M_2^-$).

The formalism used to calculate QCD corrections in this case is analogous to the one developed in Ref. [46] in the context of $0\nu\beta\beta$ -decay, based in Refs. [51,61]. Here we briefly discuss the differences and additional aspects that need to be taken into account for the processes studied in this work. The flavour configuration in the quark-level Lagrangian of $0\nu\beta\beta$ -decay is composed by only two quark flavors (u and d), having schematically operators of the form $(\bar{u}\Gamma_1 d)(\bar{u}\Gamma_2 d) \cdot j_\ell$, with Γ_1, Γ_2 representing in general different Lorentz structures, and j_ℓ the leptonic current, which is irrelevant from the QCD point of view in the case of $0\nu\beta\beta$ -decay, but not in the general case where the chirality of the tensor lepton current does impact operator mixing, as we will see. Fierz transformations and mixing under renormalization of these kind of operators lead back to the same flavor structure $(\bar{u}\Gamma_1 d)(\bar{u}\Gamma_2 d)$ but with the consequent mixing between different Lorentz structures. This is not necessarily the case for the operators that contribute to $M_1^- \rightarrow M_2^+ \ell_1^- \ell_2^-$ and $\tau^- \rightarrow \ell^+ M_1^- M_2^-$ decays. Depending on the specific process under consideration, a generally non-invariant flavor structure under Fierz transformation can result in mixing not only among operators with different Lorentz structures but also with distinct flavor configurations. Such behavior leads to anomalous dimension and μ -evolution matrices that are, in general, of larger size than those in the $0\nu\beta\beta$ -decay case. From the perspective of meson decays, this implies that after hadronization, mixing will emerge between operators contributing to the decay of different mesons. Considering that the constraints on distinct decays generally vary, new bounds can be established due to this mixing.

Additionally, in the $M_1^- \rightarrow M_2^+ \ell_1^- \ell_2^-$ and $\tau^- \rightarrow \ell^+ M_1^- M_2^-$ decays, the matrix elements of operators that contain a tensor quark current (i.e., $\mathcal{O}_{2,4,7,8}$) vanish at first order after hadronization [44,60], therefore these operators are not bounded at the tree-level. However, given that QCD corrections can mix the tensor quark operators ($\mathcal{O}_{2,4,7,8}$) at the quark level, residual contributions from these WCs ($C_{2,4,7,8}$) appear in the QCD-corrected partial decay width formulas. This means that not only improved limits on WCs are found by considering QCD corrections, but also new limits on tensor operators not constrained at the tree-level.

Figures (1) and (2) show the one-loop QCD corrections applied to the meson and tau decays, respectively.³ As it is well-known [46], operator mixing under renormalization appears given the existence of a non-diagonal renormalization matrix. Equivalently, this mixing can be understood as a mixing between the WCs.

Using the renormalization group (RG) equation formalism outlined for $0\nu\beta\beta$ -decay in Ref. [46], the RG equation for the WCs is the following:

$$\frac{d\vec{C}(\mu)}{d\ln\mu} = \hat{\gamma}^T \vec{C}(\mu). \quad (24)$$

³In this work, we consider the RGE evolution driven by QCD corrections below the electroweak scale, specifically from $\Lambda = m_Z$ to $\mu = 1$ GeV. Although electroweak corrections above the m_Z scale, of order $\mathcal{O}(\alpha_2/4\pi)$, are beyond the scope of this study and are comparatively small relative to QCD corrections, they may still be of interest due to the additional mixing effects they can induce, particularly with operators relevant to $0\nu\beta\beta$ decay.

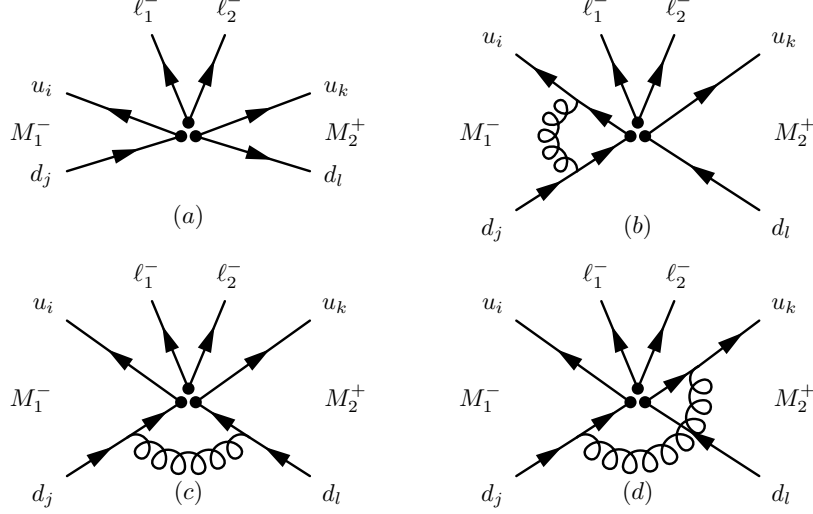


Figure 1: Effective $d = 9$ operator description of the short-range mechanisms (SRM) of the meson decay $M_1^- \rightarrow M_2^+ \ell_1^- \ell_2^-$. Diagram (a) gives the tree-level description, while diagrams (b)-(d) are one-loop QCD corrections to the amplitude.

Here, the vector $\vec{C} = (C_1, C_2, \dots)$ contains the Wilson coefficients, and $\hat{\gamma}^T$ is the transposed anomalous dimension matrix. The solution to Eq. (24) is given by:

$$\vec{C}(\mu) = \hat{U}(\mu, \Lambda) \cdot \vec{C}(\Lambda), \quad (25)$$

where $\hat{U}(\mu, \Lambda)$ serves as an evolution matrix linking the high-energy scale Λ and the low-energy scale μ .

At leading order (LO), the evolution matrix is:

$$\hat{U}(\mu, \Lambda) = \hat{V} \text{Diag} \left\{ \left(\frac{\alpha_s(\Lambda)}{\alpha_s(\mu)} \right)^{\hat{\gamma}/(2\beta_0)} \right\} \hat{V}^{-1}, \quad (26)$$

where the LO QCD running coupling constant is:

$$\alpha_s(\mu) = \frac{\alpha_s(\Lambda)}{1 - \frac{\beta_0 \alpha_s(\Lambda)}{2\pi} \log \left(\frac{\Lambda}{\mu} \right)}. \quad (27)$$

Here, $\beta_0 = (33 - 2f)/3$, where f denotes the number of quark flavors with masses $m_f < \mu$. We normalize using the value of α_s at the scale of the Z -boson mass: $\alpha_s(\mu = m_z) = 0.118$ [62]. The matrix \hat{V} in Eq. (26) is defined as:

$$\hat{\gamma}_D = \hat{V}^{-1} \hat{\gamma}^T \hat{V}, \quad (28)$$

where $\hat{\gamma}$ is the anomalous dimension matrix, whose matrix elements are:

$$(\hat{\gamma})_{ij} = \frac{\alpha_s}{4\pi} \left[-2(\hat{b}_{ij} - 2C_F \delta_{ij}) \right], \quad (29)$$

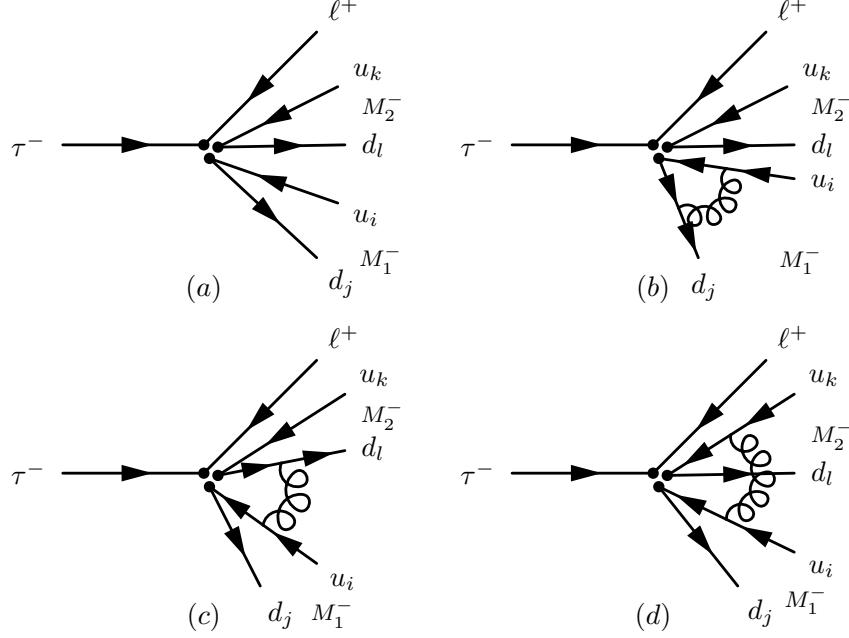


Figure 2: Effective $d = 9$ operator description of the short range mechanisms (SRM) of the decay $\tau^- \rightarrow \ell^+ M_1^- M_2^-$. Diagram (a) gives the tree-level description, while diagrams (b)-(d) are one-loop QCD corrections to the amplitude.

with $C_F = \frac{N^2-1}{2N}$ the standard $SU(N)$ color factor and the matrix \hat{b}_{ij} is derived from the one-loop QCD corrections of the operator basis [Eqs. (2)-(9)]. The general expression for the one-loop QCD-corrected operator matrix elements at LO is:

$$\langle \mathcal{O}_i \rangle^{(0)} = \left[\delta_{ij} + \frac{\alpha_s}{4\pi} b_{ij} \left(\frac{1}{\epsilon} + \ln \frac{\mu^2}{-p^2} \right) \right] \langle \mathcal{O}_j \rangle^{tree}, \quad (30)$$

where $\langle \mathcal{O}_j \rangle^{tree}$ are the tree-level operator matrix elements. For further details on the renormalization procedure for $d = 9$ effective operators with two quark currents, the reader is referred to Ref. [46].

Since due to Fierz transformations RG evolution can mix operators with different quark flavor configurations, we introduce the following notation in order to specify the different mixings in the anomalous dimension matrices. If $ijkl = 1234$ are the quark flavor indices of the operator \mathcal{O}_n , then we define the following permutations of the quark flavor indices:

$$\mathcal{O}'_{n(1234)} = \mathcal{O}_{n(1432)}, \quad \overline{\mathcal{O}}^{XYZ}_{n(1234)} = \mathcal{O}_{n(3412)}^{XYZ}, \quad \overline{\mathcal{O}}^{XYZ}_{n(1234)} = \mathcal{O}_{n(3214)}^{XYZ}. \quad (31)$$

Therefore, for example, the anomalous dimension matrix $\hat{\gamma}_{13'}^{XYZ}(ijkl)$ mixes operators $\mathcal{O}_{1(ijkl)}^{XYZ}$ and $\mathcal{O}'_{3(ijkl)} = \mathcal{O}_{3(ilkj)}^{XYZ}$. Note that for operators with repeated u -type quarks ($i = k$), $\mathcal{O} = \overline{\mathcal{O}'}$ and $\mathcal{O}' = \overline{\mathcal{O}}$, while operators with repeated d -type quarks ($j = l$) satisfy $\mathcal{O} = \mathcal{O}'$ and $\overline{\mathcal{O}} = \overline{\mathcal{O}'}$. On the other hand, for operators involving four different quark flavors ($i \neq k, j \neq l$), the operators \mathcal{O} , \mathcal{O}' , $\overline{\mathcal{O}}$, and $\overline{\mathcal{O}'}$ are all different.

The anomalous dimension matrices are listed next. They are denoted by $\hat{\gamma}_{n_1 n_2, \dots}^{XYZ}(ijkl)$, where $n_1 n_2, \dots$ represent the operators $\mathcal{O}_{n_1}, \mathcal{O}_{n_2}, \dots$ mixed by the anomalous dimension matrix, XYZ the chiralities of the operators, and the indices $i, k = u, c$, and $j, l = d, s, b$

represent quark flavors. We group the anomalous dimensions in four groups depending on the symmetry of their flavor indices ($ijkl$): (i) Repeated up-flavor quarks, (ii) repeated down-flavor quarks, (iii) repeated up- and down-flavor quarks, (iv) all quark flavors different. Unless explicitly indicated, in the matrices below the flavor indices ($ijkl$) are all different.

Repeated up-flavor quarks ($i = k$):

$$\hat{\gamma}_{(12)}^{XXZ}(ijil) = -2 \begin{pmatrix} 6C_F - 3 & \frac{N-2}{4N} \\ -\frac{12(2+N)}{N} & -3 - 2C_F \end{pmatrix}, \quad \hat{\gamma}_{(13)}^{(LR/RL)Z}(ijil) = -2 \begin{pmatrix} 6C_F & 0 \\ -6 & -\frac{3}{N} \end{pmatrix}, \quad (32)$$

$$\hat{\gamma}_{(13)}^{(LR/RL)Z}(ijil) = -2 \begin{pmatrix} 6C_F & 0 \\ -6 & -\frac{3}{N} \end{pmatrix}, \quad \hat{\gamma}_{(3)}^{XXZ}(ijil) = -2 \left(-3 + \frac{3}{N} \right) \quad (33)$$

$$\hat{\gamma}_{(44'55')}^{XXZ}(ijil) = -2 \begin{pmatrix} -C_F & -\frac{3}{2} & -\frac{3i}{N} & -\frac{3i}{2} \\ -\frac{3}{2} & -C_F & -\frac{3i}{2} & -\frac{3i}{N} \\ \frac{i}{N} & -\frac{i}{2} & 3C_F & -\frac{3}{2} \\ -\frac{i}{2} & \frac{i}{N} & -\frac{3}{2} & 3C_F \end{pmatrix}, \quad (34)$$

$$\hat{\gamma}_{(45)}^{(LR/RL)Z}(ijil) = -2 \begin{pmatrix} -\frac{3}{2} - C_F & \frac{3i(N+2)}{2N} \\ \frac{i(N-2)}{2N} & -\frac{3}{2} + 3C_F \end{pmatrix}, \quad (35)$$

$$\hat{\gamma}_{(6)}^{XXX}(ijil) = -2 \left(-1 + \frac{1}{N} \right), \quad \hat{\gamma}_{(6)}^{LLR/RRL}(ijil) = -2 \left(1 + \frac{1}{N} \right), \quad (36)$$

$$\hat{\gamma}_{(67)}^{LRR/RLL}(ijil) = -2 \begin{pmatrix} -\frac{1}{N} & \frac{i}{2} \\ 0 & 2C_F \end{pmatrix}, \quad (37)$$

$$\hat{\gamma}_{(778)}^{XXX}(ijil) = -2 \begin{pmatrix} 2C_F - \frac{1}{N} - 2 & -\frac{1}{N} & -\frac{i(8+N)}{8N} \\ -\frac{1}{N} & 2C_F - \frac{1}{N} - 2 & \frac{i(8+N)}{8N} \\ 0 & 0 & -2C_F \end{pmatrix}. \quad (38)$$

Repeated down-flavor quarks ($j = l$):

$$\hat{\gamma}_{(12)}^{XXZ}(ijkj) = -2 \begin{pmatrix} 6C_F - 3 & \frac{N-2}{4N} \\ -\frac{12(2+N)}{N} & -3 - 2C_F \end{pmatrix}, \quad (39)$$

$$\hat{\gamma}_{(13)}^{(LR/RL)Z}(ijkj) = -2 \begin{pmatrix} 6C_F & 0 \\ -6 & -\frac{3}{N} \end{pmatrix}, \quad \hat{\gamma}_{(3)}^{XXZ}(ijkj) = -2 \left(-3 + \frac{3}{N} \right) \quad (40)$$

$$\hat{\gamma}_{(45)}^{XXZ}(ijkj) = -2 \begin{pmatrix} -\frac{3}{2} - C_F & -\frac{3i(N+2)}{2N} \\ -\frac{i(N-2)}{2N} & -\frac{3}{2} + 3C_F \end{pmatrix}, \quad (41)$$

$$\hat{\gamma}_{(4455)}^{(LR/RL)Z}(ijkj) = -2 \begin{pmatrix} -C_F & -\frac{3}{2} & \frac{3i}{N} & \frac{3i}{2} \\ -\frac{3}{2} & -C_F & \frac{3i}{2} & \frac{3i}{N} \\ -\frac{i}{N} & \frac{i}{2} & 3C_F & -\frac{3}{2} \\ \frac{i}{2} & -\frac{i}{N} & -\frac{3}{2} & 3C_F \end{pmatrix}, \quad (42)$$

$$\hat{\gamma}_{(6)}^{XXX}(ijkj) = -2 \left(1 + \frac{1}{N}\right), \quad \hat{\gamma}_{(6)}^{LLR/RRL}(ijkj) = -2 \left(-1 + \frac{1}{N}\right), \quad (43)$$

$$\hat{\gamma}_{(6\bar{7})}^{LRR/RLL}(ijkj) = -2 \begin{pmatrix} -\frac{1}{N} & \frac{i}{2} \\ 0 & 2C_F \end{pmatrix}, \quad (44)$$

$$\hat{\gamma}_{(7\bar{7}8)}^{XXX}(ijkj) = -2 \begin{pmatrix} 2C_F - \frac{1}{N} & -2 - \frac{1}{N} & \frac{i(N-8)}{8N} \\ -2 - \frac{1}{N} & 2C_F - \frac{1}{N} & -\frac{i(N-8)}{8N} \\ 0 & 0 & -2C_F \end{pmatrix}. \quad (45)$$

Repeated up- and down-flavor quarks ($i = k, j = l$):⁴

$$\hat{\gamma}_{(12)}^{XXZ}(ijij) = -2 \begin{pmatrix} 6C_F - 3 & \frac{N-2}{4N} \\ -\frac{12(2+N)}{N} & -3 - 2C_F \end{pmatrix}, \quad \hat{\gamma}_{(13)}^{(LR/RL)Z}(ijij) = -2 \begin{pmatrix} 6C_F & 0 \\ -6 & -\frac{3}{N} \end{pmatrix}, \quad (46)$$

$$\hat{\gamma}_{(3)}^{XXZ}(ijij) = -2 \left(-3 + \frac{3}{N}\right), \quad \hat{\gamma}_{(45)}^{XXZ}(ijij) = -2 \begin{pmatrix} -\frac{3}{2} - C_F & -\frac{3i(N+2)}{2N} \\ -\frac{i(N-2)}{2N} & -\frac{3}{2} + 3C_F \end{pmatrix}, \quad (47)$$

$$\hat{\gamma}_{(45)}^{(LR/RL)Z}(ijij) = -2 \begin{pmatrix} -\frac{3}{2} - C_F & \frac{3i(N+2)}{2N} \\ \frac{i(N-2)}{2N} & -\frac{3}{2} + 3C_F \end{pmatrix}, \quad (48)$$

$$\hat{\gamma}_{(67)}^{LRR/RLL}(ijij) = -2 \begin{pmatrix} -\frac{1}{N} & \frac{i}{2} \\ 0 & 2C_F \end{pmatrix}, \quad (49)$$

$$\hat{\gamma}_{(7)}^{XXX}(ijij) = -2 \left(-2 + 2C_F - \frac{2}{N}\right) = 0, \quad (\text{for } N = 3). \quad (50)$$

All quark flavors different:

$$\hat{\gamma}_{(11'22')}^{XXZ}(ijkl) = -2 \begin{pmatrix} 6C_F & -3 & -\frac{1}{2N} & \frac{1}{4} \\ -3 & 6C_F & \frac{1}{4} & -\frac{1}{2N} \\ -\frac{24}{N} & -12 & -2C_F & -3 \\ -12 & -\frac{24}{N} & -3 & -2C_F \end{pmatrix}, \quad (51)$$

⁴This case, excepting for the possibility of different lepton flavors, is similar to the RG evolution of the operators involved in the short-range mechanism of $0\nu\beta\beta$ -decay. This is relevant for the decays $\tau^- \rightarrow \ell^+ M_1^- M_2^-$, with $M_1^- = M_2^-$.

$$\hat{\gamma}_{(13')}^{(LR/RL)Z}(ijkl) = -2 \begin{pmatrix} 6C_F & 0 \\ -6 & -\frac{3}{N} \end{pmatrix}, \quad \hat{\gamma}_{(33')}^{XXZ}(ijkl) = -2 \begin{pmatrix} \frac{3}{N} & -3 \\ -3 & \frac{3}{N} \end{pmatrix}, \quad (52)$$

$$\hat{\gamma}_{(44'55')}^{XXZ}(ijkl) = -2 \begin{pmatrix} -C_F & -\frac{3}{2} & -\frac{3i}{N} & -\frac{3i}{2} \\ -\frac{3}{2} & -C_F & -\frac{3i}{2} & -\frac{3i}{N} \\ \frac{i}{N} & -\frac{i}{2} & 3C_F & -\frac{3}{2} \\ -\frac{i}{2} & \frac{i}{N} & -\frac{3}{2} & 3C_F \end{pmatrix}, \quad (53)$$

$$\hat{\gamma}_{(44'55')}^{(LR/RL)Z}(ijkl) = -2 \begin{pmatrix} -C_F & -\frac{3}{2} & \frac{3i}{N} & \frac{3i}{2} \\ -\frac{3}{2} & -C_F & \frac{3i}{2} & \frac{3i}{N} \\ -\frac{i}{N} & \frac{i}{2} & 3C_F & -\frac{3}{2} \\ \frac{i}{2} & -\frac{i}{N} & -\frac{3}{2} & 3C_F \end{pmatrix}, \quad (54)$$

$$\hat{\gamma}_{(66')}^{XXX}(ijkl) = -2 \begin{pmatrix} \frac{1}{N} & 1 \\ 1 & \frac{1}{N} \end{pmatrix}, \quad \hat{\gamma}_{(66')}^{LLR/RLL}(ijkl) = -2 \begin{pmatrix} \frac{1}{N} & -1 \\ -1 & \frac{1}{N} \end{pmatrix}, \quad (55)$$

$$\hat{\gamma}_{(67)}^{LLR/RLL}(ijkl) = -2 \begin{pmatrix} -\frac{1}{N} & \frac{i}{2} \\ 0 & 2C_F \end{pmatrix}, \quad (56)$$

$$\hat{\gamma}_{(77'77'88')}^{XXX}(ijkl) = -2 \begin{pmatrix} 2C_F - \frac{1}{N} & 0 & -\frac{1}{N} & -2 & -\frac{i}{N} & \frac{i}{8} \\ 0 & 2C_F - \frac{1}{N} & -2 & -\frac{1}{N} & \frac{i}{8} & -\frac{i}{N} \\ -\frac{1}{N} & -2 & 2C_F - \frac{1}{N} & 0 & \frac{i}{N} & -\frac{i}{8} \\ -2 & -\frac{1}{N} & 0 & 2C_F - \frac{1}{N} & -\frac{i}{8} & \frac{i}{N} \\ 0 & 0 & 0 & 0 & -2C_F & 0 \\ 0 & 0 & 0 & 0 & 0 & -2C_F \end{pmatrix}. \quad (57)$$

From the previous anomalous dimension matrices, Eqs.(32)-(57) and the definition of $\hat{U}(\mu, \Lambda)$ in Eq. (26), we obtain the μ -evolution matrices for the RG evolution from $\Lambda = m_Z$ to $\mu = 1 \text{ GeV}$. It is important to account for the quark thresholds when considering the evolution of the Wilson coefficients. To address this, we consider consecutive μ -evolution matrices, each corresponding to a different number (f) of quark flavors:

$$\hat{U}(\mu, \Lambda = m_Z) = \hat{U}^{(f=3)}(\mu, \mu_c) \hat{U}^{(f=4)}(\mu_c, \mu_b) \hat{U}^{(f=5)}(\mu_b, m_Z), \quad (58)$$

where the intermediate scales are the corresponding quark masses ($\mu_c = m_c$, $\mu_b = m_b$). This evolution matrices will be used in the next section and are listed in Appendix (A).

4 RGE-Induced Bounds on Wilson Coefficients

In this section, we derive RGE-improved bounds on the Wilson coefficients ($C_{n(ijkl)}^{XYZ}$), which are associated with the dimension-9 operator basis listed in Eqs.(2)-(9). These operators contribute to the LNV meson decays $M_1^- \rightarrow M_2^+ \ell_1^- \ell_2^-$ and to the LNV tau decays

$\tau^- \rightarrow \ell^+ M_1^- M_2^-$. Many of these processes have been searched experimentally, and their non-observation puts upper bounds on their branching fractions. The existing experimental limits on the branching fractions for different LNV meson and tau decay are shown in Tables (1) and (2).

Using the expressions for the partial widths given in Eqs. (17) and (21) for meson and tau decays in terms of the Wilson coefficients, we can translate the experimental bounds listed in Tables (1) and (2) into constraints on the respective Wilson coefficients. The resultant bounds are presented in Tables (3)-(12) under the ‘‘Tree Level’’ column, as they do not take into account RG evolution effects. We can see that the most stringent tree-level bounds on the Wilson coefficients stem from the LNV kaon and B -meson decays $K^- \rightarrow \pi^+ \ell_1^- \ell_2^-$ and $B^- \rightarrow \pi^+ \mu^- \mu^-$ [of order $\mathcal{O}(1)$ and $\mathcal{O}(10^2)$ respectively] since these processes have the strongest experimental bounds (see Table 1). The remaining processes translate into tree-level bounds of the Wilson coefficients up to three orders of magnitude weaker.⁵

The RG evolution matrices $U(\mu, \Lambda)$, calculated in Sec. (3) and listed in Appendix (A), allow us to derive new limits on the Wilson coefficients. If at the tree level the Wilson coefficient C_n appearing in the expressions for the partial decay widths [Eqs. (17) and (21)] has a tree-level bound $C_n \lesssim C_n^{exp}$, then due to radiative corrections, the tree-level Wilson coefficient C_n should be replaced by $C_n(\mu)$ according to Eq. (25), i.e,

$$C_n \rightarrow C_n(\mu) = \sum_m \hat{U}_{nm}(\mu, \Lambda) C_m(\Lambda) \lesssim C_n^{exp}, \quad (59)$$

where the indices n, m run over the operators that are mixed by the evolution matrix $\hat{U}(\mu, \Lambda)$. In order to extract the RGE improved bounds from Eq. (59), we apply the conventional assumption about the presence of only one operator at a time in the sum in Eq. (59). These simplified ‘‘*on-axis*’’ limits on $C_n(\Lambda)$ are shown in Tables (3)-(12) under the columns labeled ‘‘With QCD Corrections’’. The numerical values of the constants used in the calculations are listed in Appendix (B).

The most notable results are the new induced bounds on operators that are not constrained at the tree level. This is the case for operators \mathcal{O}_2 , \mathcal{O}_4 , and \mathcal{O}_7 , whose respective RGE-induced bounds are shown in gray-color background in Tables (3), (5), and (7) for meson decays, and in Tables (8), (10), and (12) for tau decays. It can be seen from the evolution matrices in Appendix (A) that these new bounds on C_2 , C_4 , and C_7 , are inherited due to mixing from the tree-level bounds on C_1 , C_5 , and C_6 , respectively.

In Sec. (3), we found that the RG evolution for operators $\mathcal{O}_{n(ijkl)}^{XYZ}$ with different flavor quarks ($i \neq j \neq k \neq l$) also induces mixing with operators with different quarks flavor configurations (i.e., the \mathcal{O}' , $\overline{\mathcal{O}}$, and $\overline{\mathcal{O}'}$ operators defined in Eq. (31)). These mixings also induce bounds on operators not constrained at the tree level, as is the case of the bounds coming from the processes $B^- \rightarrow D^+ \ell_1^- \ell_2^-$ and $B^- \rightarrow D_s^+ \mu^- \mu^-$. At the tree level, these processes constrain the operators $\mathcal{O}_{n(ubcd)}^{XYZ(\ell_1 \ell_2)}$ and $\mathcal{O}_{n(ubcs)}^{XYZ(\mu\mu)}$, respectively, while due to RGE effects they also induce bounds on $\mathcal{O}_{n(udcb)}^{XYZ(\ell_1 \ell_2)}$ and $\mathcal{O}_{n(uscb)}^{XYZ(\mu\mu)}$, as shown in Tables (3)-(6).

Note that the operators bounded by the processes $D^- \rightarrow K^+ \ell_1^- \ell_2^-$ and $D_s^- \rightarrow \pi^+ \ell_1^- \ell_2^-$ mix under RG evolution, so these processes put bounds on the same set of operators. For this

⁵This range of bounds on the Wilson coefficients (C_n) translated into the new physics scale Λ_{NP} (through $1/\Lambda_{NP}^5 = C_n G_F^2/2m$) corresponds to $\Lambda_{NP} \gtrsim (8 - 94) \text{ GeV}$.

reason, when we inform the bounds on the Wilson coefficients associated to these processes, for comparison purposes we use the average mass of the D^- and D_s^- mesons for the mass scale m appearing in the definition of the Wilson coefficient [see Eq. (1)].

Additionally, we find that the bounds on the Wilson coefficients C_1^{XXZ} and $C_1^{(LR,RL)Z}$ are improved by a factor of ~ 2 and ~ 3 , respectively, as can be seen in Tables (3) and (8).

5 Summary and Conclusions

In this work, we calculate RGE-improved bounds on the Wilson coefficients of the LNV ($\Delta L = 2$) low energy effective Lagrangian presented in Sec. (2). A subset of these operators, particularly $\mathcal{O}_{1,2,3,4,5}$ with first-generation quarks and leptons, contributes to the short-range mechanism of $0\nu\beta\beta$ -decay, and therefore they are strongly constrained. Operators with other quark or lepton flavor content (which are not constrained by $0\nu\beta\beta$ -decay) are bounded by the non-observation of different LNV meson and tau decays.

We calculate QCD corrections to this operator basis and find the RG evolution matrices, which show how the Wilson coefficients evolve from one energy scale to another. Unlike the $0\nu\beta\beta$ case studied in the literature, here the general flavor structure results in the mixing of not only different Lorentz structures but also distinct quark flavor configurations. This implies that after hadronization there can be mixing between operators responsible for the decay of distinct mesons, leading to new bounds on certain operators (e.g., the operators contributing to $D^- \rightarrow K^+\ell^-\ell^-$ and $D_s^- \rightarrow \pi^+\ell^-\ell^-$).

We use the existing experimental limits on 3-body LNV meson and tau decays [shown in Tables (1) and (2)] and the expressions for their partial decay widths in terms of the corresponding Wilson coefficients, to convert these experimental bounds into constraints on the Wilson coefficients. Then we use the RG evolution matrices calculated in section (3) to derive QCD-improved bounds on the Wilson coefficients. Tables (3)-(12) show our results under the column ‘‘With QCD Corrections’’. For comparison, we include the tree-level results under the column ‘‘Tree Level’’.

One of the significant findings are the new constraints on certain operators that were not bounded at the tree level. This was the case for operators \mathcal{O}_2 , \mathcal{O}_4 , and \mathcal{O}_7 . Furthermore, the RG evolution led to the mixing of certain operators with operators of a different quark-flavor configuration. As a result, new constraints appear on operators that were not initially constrained, as is the case for operators contributing to $B^- \rightarrow D^+\ell_1^-\ell_2^-$ and $B^- \rightarrow D_s^+\mu^-\mu^-$. Additionally, we found that RG evolution improves the bounds on the Wilson coefficients C_1^{XXZ} and $C_1^{(LR/RL)Z}$ by factors of 2 and 3, respectively, excepting for the operators contributing $D^- \rightarrow K^+\ell_1^-\ell_2^-$ and $D_s^- \rightarrow \pi^+\ell_1^-\ell_2^-$, where the improvement can be up to a factor of 20.

Process	$(ij)(kl)(\ell_1\ell_2)$	Tree Level		With QCD Corrections		
		$C_{1(ijkl)}^{XYZ}$	$C_{2(ijkl)}^{XXX}$	$C_{1(ijkl)}^{XXZ}$	$C_{1(ijkl)}^{(LR,RL)Z}$	$C_{2(ijkl)}^{XXX}$
$K^- \rightarrow \pi^+ e^- e^-$	$(us)(ud)(ee)$	2.0	–	9.9×10^{-1}	6.5×10^{-1}	2.0×10^2
$D^- \rightarrow \pi^+ e^- e^-$	$(cd)(ud)(ee)$	4.8×10^3	–	2.4×10^3	1.6×10^3	4.8×10^5
$D^- \rightarrow K^+ e^- e^-$	$(cd)(us)(ee)$	9.3×10^3	–	2.8×10^3	3.1×10^3	1.5×10^5
$D_s^- \rightarrow \pi^+ e^- e^-$	$(cs)(ud)(ee)$	8.3×10^3	–	2.5×10^3	2.7×10^3	1.3×10^5
$D_s^- \rightarrow K^+ e^- e^-$	$(cs)(us)(ee)$	8.9×10^3	–	4.5×10^3	2.9×10^3	1.2×10^5
$B^- \rightarrow \pi^+ e^- e^-$	$(ub)(ud)(ee)$	2.0×10^2	–	1.0×10^2	6.7×10^1	2.0×10^4
$B^- \rightarrow K^+ e^- e^-$	$(ub)(us)(ee)$	2.4×10^2	–	1.2×10^2	7.8×10^1	2.4×10^4
$B^- \rightarrow D^+ e^- e^-$	$(ub)(cd)(ee)$	2.9×10^3	–	8.8×10^2	9.5×10^2	4.8×10^4
	$(ud)(cb)(ee)$	–	–	2.2×10^3	2.9×10^3	4.1×10^4
$K^- \rightarrow \pi^+ \mu^- \mu^-$	$(us)(ud)(\mu\mu)$	2.9	–	1.5	9.7×10^{-1}	2.9×10^2
$D^- \rightarrow \pi^+ \mu^- \mu^-$	$(cd)(ud)(\mu\mu)$	7.9×10^2	–	4.0×10^2	2.6×10^2	7.9×10^4
$D^- \rightarrow K^+ \mu^- \mu^-$	$(cd)(us)(\mu\mu)$	3.2×10^4	–	1.6×10^3	1.1×10^4	3.0×10^4
$D_s^- \rightarrow \pi^+ \mu^- \mu^-$	$(cs)(ud)(\mu\mu)$	2.1×10^3	–	6.4×10^2	6.9×10^2	3.5×10^4
$D_s^- \rightarrow K^+ \mu^- \mu^-$	$(cs)(us)(\mu\mu)$	1.7×10^3	–	8.4×10^2	5.5×10^2	1.7×10^5
$B^- \rightarrow \pi^+ \mu^- \mu^-$	$(ub)(ud)(\mu\mu)$	8.5×10^1	–	4.3×10^1	2.8×10^1	8.5×10^3
$B^- \rightarrow K^+ \mu^- \mu^-$	$(ub)(us)(\mu\mu)$	2.8×10^2	–	1.4×10^2	9.2×10^1	2.8×10^4
$B^- \rightarrow D^+ \mu^- \mu^-$	$(ub)(cd)(\mu\mu)$	1.5×10^3	–	4.6×10^2	4.9×10^2	2.5×10^4
	$(ud)(cb)(\mu\mu)$	–	–	1.2×10^3	1.5×10^3	2.1×10^4
$B^- \rightarrow D_s^+ \mu^- \mu^-$	$(ub)(cs)(\mu\mu)$	1.2×10^3	–	3.7×10^2	3.9×10^2	2.0×10^4
	$(us)(cb)(\mu\mu)$	–	–	9.3×10^2	1.2×10^3	1.7×10^4
$K^- \rightarrow \pi^+ e^- \mu^-$	$(us)(ud)(e\mu)$	1.5	–	7.7×10^{-1}	5.1×10^{-1}	1.5×10^2
$D^- \rightarrow \pi^+ e^- \mu^-$	$(cd)(ud)(e\mu)$	1.7×10^3	–	8.5×10^2	5.6×10^2	1.7×10^5
$D^- \rightarrow K^+ e^- \mu^-$	$(cd)(us)(e\mu)$	9.7×10^3	–	3.0×10^3	3.2×10^3	5.7×10^4
$D_s^- \rightarrow \pi^+ e^- \mu^-$	$(cs)(ud)(e\mu)$	4.0×10^3	–	1.2×10^3	1.3×10^3	6.6×10^4
$D_s^- \rightarrow K^+ e^- \mu^-$	$(cs)(us)(e\mu)$	3.7×10^3	–	1.9×10^3	1.2×10^3	3.7×10^5
$B^- \rightarrow \pi^+ e^- \mu^-$	$(ub)(ud)(e\mu)$	3.7×10^2	–	1.9×10^2	1.2×10^2	3.7×10^4
$B^- \rightarrow K^+ e^- \mu^-$	$(ub)(us)(e\mu)$	3.9×10^2	–	2.0×10^2	1.3×10^2	3.9×10^4
$B^- \rightarrow D^+ e^- \mu^-$	$(ub)(cd)(e\mu)$	1.7×10^3	–	5.2×10^2	5.6×10^2	2.8×10^4
	$(ud)(cb)(e\mu)$	–	–	1.3×10^3	1.7×10^3	2.4×10^4

Table 3: Upper bounds on the Wilson coefficients $C_{1(ijkl)}^{XYZ(\ell_1\ell_2)}$ and $C_{2(ijkl)}^{XXX(\ell_1\ell_2)}$ extracted from the experimental limits on the LNV meson decays $M_1 \rightarrow M_2 \ell_1^- \ell_2^-$ shown in Table (1), with and without QCD corrections. The bounds in gray background are new results present only after including the effects of QCD corrections. The bounds which improve by at least a factor of 2 with respect to the corresponding tree-level bound are shown in light-gray. Note that the operators bounded by the processes $D^- \rightarrow K^+ \ell_1^- \ell_2^-$ and $D_s^- \rightarrow \pi^+ \ell_1^- \ell_2^-$ mix under RG evolution, so these processes put bounds on the same sets of operators.

Process	$(ij)(kl)(\ell_1\ell_2)$	Tree Level	With QCD Corrections	
		$C_{3(ijkl)}^{XYZ}$	$C_{3(ijkl)}^{XXZ}$	$C_{3(ijkl)}^{(LR,RL)Z}$
$K^- \rightarrow \pi^+ e^- e^-$	$(us)(ud)(ee)$	1.5×10^2	1.9×10^2	1.7×10^2
$D^- \rightarrow \pi^+ e^- e^-$	$(cd)(ud)(ee)$	3.7×10^4	4.8×10^4	4.2×10^4
$D^- \rightarrow K^+ e^- e^-$	$(cd)(us)(ee)$	4.8×10^4	3.8×10^4	5.5×10^4
$D_s^- \rightarrow \pi^+ e^- e^-$	$(cs)(ud)(ee)$	6.0×10^4	4.8×10^4	6.9×10^4
$D_s^- \rightarrow K^+ e^- e^-$	$(cs)(us)(ee)$	4.4×10^4	5.7×10^4	5.0×10^4
$B^- \rightarrow \pi^+ e^- e^-$	$(ub)(ud)(ee)$	5.0×10^2	6.6×10^2	5.8×10^2
$B^- \rightarrow K^+ e^- e^-$	$(ub)(us)(ee)$	4.8×10^2	6.4×10^2	5.6×10^2
$B^- \rightarrow D^+ e^- e^-$	$(ub)(cd)(ee)$	4.2×10^3	3.4×10^3	4.8×10^3
	$(ud)(cb)(ee)$	–	8.6×10^3	–
$K^- \rightarrow \pi^+ \mu^- \mu^-$	$(us)(ud)(\mu\mu)$	2.4×10^2	3.2×10^2	2.8×10^2
$D^- \rightarrow \pi^+ \mu^- \mu^-$	$(cd)(ud)(\mu\mu)$	6.2×10^3	8.1×10^3	7.1×10^3
$D^- \rightarrow K^+ \mu^- \mu^-$	$(cd)(us)(\mu\mu)$	1.7×10^5	3.3×10^4	1.9×10^5
$D_s^- \rightarrow \pi^+ \mu^- \mu^-$	$(cs)(ud)(\mu\mu)$	1.5×10^4	1.2×10^4	1.8×10^4
$D_s^- \rightarrow K^+ \mu^- \mu^-$	$(cs)(us)(\mu\mu)$	8.3×10^3	1.1×10^4	9.5×10^3
$B^- \rightarrow \pi^+ \mu^- \mu^-$	$(ub)(ud)(\mu\mu)$	2.1×10^2	2.8×10^2	2.4×10^2
$B^- \rightarrow K^+ \mu^- \mu^-$	$(ub)(us)(\mu\mu)$	5.7×10^2	7.5×10^2	6.5×10^2
$B^- \rightarrow D^+ \mu^- \mu^-$	$(ub)(cd)(\mu\mu)$	2.2×10^3	1.7×10^3	2.5×10^3
	$(ud)(cb)(\mu\mu)$	–	4.5×10^3	–
$B^- \rightarrow D_s^+ \mu^- \mu^-$	$(ub)(cs)(\mu\mu)$	1.8×10^3	1.4×10^3	2.0×10^3
	$(us)(cb)(\mu\mu)$	–	3.6×10^3	–
$K^- \rightarrow \pi^+ e^- \mu^-$	$(us)(ud)(e\mu)$	1.2×10^2	1.6×10^2	1.4×10^2
$D^- \rightarrow \pi^+ e^- \mu^-$	$(cd)(ud)(e\mu)$	1.3×10^4	1.7×10^4	1.5×10^4
$D^- \rightarrow K^+ e^- \mu^-$	$(cd)(us)(e\mu)$	5.0×10^4	4.0×10^4	5.8×10^4
$D_s^- \rightarrow \pi^+ e^- \mu^-$	$(cs)(ud)(e\mu)$	2.9×10^4	2.3×10^4	3.3×10^4
$D_s^- \rightarrow K^+ e^- \mu^-$	$(cs)(us)(e\mu)$	1.8×10^4	2.4×10^4	2.1×10^4
$B^- \rightarrow \pi^+ e^- \mu^-$	$(ub)(ud)(e\mu)$	9.1×10^2	1.2×10^3	1.0×10^3
$B^- \rightarrow K^+ e^- \mu^-$	$(ub)(us)(e\mu)$	7.9×10^2	1.0×10^3	9.1×10^2
$B^- \rightarrow D^+ e^- \mu^-$	$(ub)(cd)(e\mu)$	2.5×10^3	2.0×10^3	2.9×10^3
	$(ud)(cb)(e\mu)$	–	5.1×10^3	–

Table 4: Upper bounds on the Wilson coefficients $C_{3(ijkl)}^{XYZ(\ell_1\ell_2)}$ extracted from the experimental limits on the LNV meson decays $M_1 \rightarrow M_2 \ell_1^- \ell_2^-$ shown in Table (1), with and without QCD corrections. The bounds in gray background are new results present only after including the effects of QCD corrections. For the operators shown in this table, existing tree-level bounds are not improved by QCD effects, excepting for $C_{3(cdus)}^{XXZ(\mu\mu)}$ (in light gray) which improves due to the mixing under RG evolution of the operators contributing to the processes $D^- \rightarrow K^+ \ell_1^- \ell_2^-$ and $D_s^- \rightarrow \pi^+ \ell_1^- \ell_2^-$.

Process	$(ij)(kl)(\ell_1\ell_2)$	Tree Level		With QCD Corrections			
		$C_{4(ijkl)}^{XYZ}$	$C_{5(ijkl)}^{XYZ}$	$C_{4(ijkl)}^{XXZ}$	$C_{4(ijkl)}^{(LR,RL)Z}$	$C_{5(ijkl)}^{XXZ}$	$C_{5(ijkl)}^{(LR,RL)Z}$
$K^- \rightarrow \pi^+ e^- e^-$	$(us)(ud)(ee)$	–	1.6×10^1	1.8×10^2	8.0×10^2	9.1	1.1×10^1
	$(ud)(us)(ee)$	–	1.8×10^1	1.6×10^2	9.0×10^2	1.0×10^1	1.3×10^1
$D^- \rightarrow \pi^+ e^- e^-$	$(cd)(ud)(ee)$	–	1.3×10^4	6.7×10^5	1.4×10^5	9.5×10^3	7.6×10^3
	$(ud)(cd)(ee)$	–	1.4×10^4	7.0×10^5	1.3×10^5	9.9×10^3	7.9×10^3
$D^- \rightarrow K^+ e^- e^-$	$(cs)(ud)(ee)$	–	2.3×10^4	2.2×10^5	2.0×10^5	1.3×10^4	1.3×10^4
	$(ud)(cs)(ee)$	–	2.3×10^4	2.0×10^5	2.2×10^5	1.3×10^4	1.3×10^4
$D_s^- \rightarrow \pi^+ e^- e^-$	$(cd)(us)(ee)$	–	2.2×10^4	2.3×10^5	2.3×10^5	1.2×10^4	1.2×10^4
	$(us)(cd)(ee)$	–	2.0×10^4	2.3×10^5	2.3×10^5	1.2×10^4	1.2×10^4
$D_s^- \rightarrow K^+ e^- e^-$	$(cs)(us)(ee)$	–	2.1×10^4	1.0×10^6	1.9×10^5	1.5×10^4	1.2×10^4
	$(us)(cs)(ee)$	–	1.9×10^4	9.4×10^5	2.1×10^5	1.3×10^4	1.1×10^4
$B^- \rightarrow \pi^+ e^- e^-$	$(ub)(ud)(ee)$	–	5.1×10^2	2.2×10^3	2.6×10^4	2.9×10^2	3.6×10^2
	$(ud)(ub)(ee)$	–	2.2×10^2	2.7×10^3	1.1×10^4	1.2×10^2	1.6×10^2
$B^- \rightarrow K^+ e^- e^-$	$(ub)(us)(ee)$	–	5.6×10^2	2.2×10^3	2.8×10^4	3.2×10^2	4.0×10^2
	$(us)(ub)(ee)$	–	2.2×10^2	2.7×10^3	1.1×10^4	1.2×10^2	1.5×10^2
$B^- \rightarrow D^+ e^- e^-$	$(ub)(cd)(ee)$	–	5.4×10^3	6.8×10^4	6.8×10^4	3.1×10^3	3.1×10^3
	$(cd)(ub)(ee)$	–	2.2×10^3	2.8×10^4	2.8×10^4	1.3×10^3	1.3×10^3
	$(ud)(cb)(ee)$	–	–	5.4×10^4	2.2×10^4	1.5×10^4	6.2×10^3
	$(cb)(ud)(ee)$	–	–	2.2×10^4	5.4×10^4	6.2×10^3	1.5×10^4
$K^- \rightarrow \pi^+ \mu^- \mu^-$	$(us)(ud)(\mu\mu)$	–	3.0×10^1	3.4×10^2	1.5×10^3	1.7×10^1	2.2×10^1
	$(ud)(us)(\mu\mu)$	–	3.4×10^1	3.0×10^2	1.7×10^3	1.9×10^1	2.4×10^1
$D^- \rightarrow \pi^+ \mu^- \mu^-$	$(cd)(ud)(\mu\mu)$	–	2.3×10^3	1.1×10^5	2.4×10^4	1.6×10^3	1.3×10^3
	$(ud)(cd)(\mu\mu)$	–	2.4×10^3	1.2×10^5	2.3×10^4	1.7×10^3	1.3×10^3
$D^- \rightarrow K^+ \mu^- \mu^-$	$(cd)(us)(\mu\mu)$	–	7.7×10^4	5.9×10^4	5.9×10^4	1.6×10^4	1.6×10^4
	$(us)(cd)(\mu\mu)$	–	7.2×10^4	5.9×10^4	5.9×10^4	1.6×10^4	1.6×10^4
$D_s^- \rightarrow \pi^+ \mu^- \mu^-$	$(cs)(ud)(\mu\mu)$	–	5.9×10^3	7.3×10^4	7.3×10^5	3.3×10^3	3.3×10^3
	$(ud)(cs)(\mu\mu)$	–	5.9×10^3	7.4×10^4	7.4×10^4	3.3×10^3	3.3×10^3
$D_s^- \rightarrow K^+ \mu^- \mu^-$	$(cs)(us)(\mu\mu)$	–	4.0×10^3	2.0×10^5	3.6×10^4	2.8×10^3	2.3×10^3
	$(us)(cs)(\mu\mu)$	–	3.6×10^3	1.8×10^5	4.0×10^4	2.6×10^3	2.0×10^3
$B^- \rightarrow \pi^+ \mu^- \mu^-$	$(ub)(ud)(\mu\mu)$	–	2.1×10^2	9.2×10^2	1.1×10^4	1.2×10^2	1.5×10^2
	$(ud)(ub)(\mu\mu)$	–	9.2×10^1	1.1×10^3	4.6×10^3	5.2×10^1	6.5×10^1
$B^- \rightarrow K^+ \mu^- \mu^-$	$(ub)(us)(\mu\mu)$	–	6.6×10^2	2.5×10^3	3.3×10^4	3.7×10^2	4.7×10^2
	$(us)(ub)(\mu\mu)$	–	2.5×10^2	3.2×10^3	1.3×10^4	1.4×10^2	1.8×10^2
$B^- \rightarrow D^+ \mu^- \mu^-$	$(ub)(cd)(\mu\mu)$	–	2.8×10^3	3.5×10^4	3.5×10^4	1.6×10^3	1.6×10^3
	$(cd)(ub)(\mu\mu)$	–	1.2×10^3	1.5×10^4	1.5×10^4	6.6×10^2	6.6×10^2
	$(ud)(cb)(\mu\mu)$	–	–	2.8×10^4	1.2×10^4	7.8×10^3	3.2×10^3
	$(cb)(ud)(\mu\mu)$	–	–	1.2×10^4	2.8×10^4	3.2×10^3	7.8×10^3
$B^- \rightarrow D_s^+ \mu^- \mu^-$	$(ub)(cs)(\mu\mu)$	–	2.2×10^3	2.8×10^4	2.8×10^4	1.3×10^3	1.3×10^3
	$(cs)(ub)(\mu\mu)$	–	9.5×10^2	1.2×10^4	1.2×10^4	5.4×10^2	5.4×10^2
	$(us)(cb)(\mu\mu)$	–	–	2.2×10^4	9.5×10^3	6.2×10^3	2.6×10^3
	$(cb)(us)(\mu\mu)$	–	–	9.5×10^3	2.2×10^4	2.6×10^3	6.2×10^3
$K^- \rightarrow \pi^+ e^- \mu^-$	$(us)(ud)(e\mu)$	–	1.4×10^1	1.6×10^2	6.9×10^2	7.8	9.8
	$(ud)(us)(e\mu)$	–	1.6×10^1	1.4×10^2	7.8×10^2	8.8	1.1×10^1
$D^- \rightarrow \pi^+ e^- \mu^-$	$(cd)(ud)(e\mu)$	–	4.8×10^3	2.4×10^5	5.0×10^4	3.4×10^3	2.7×10^3
	$(ud)(cd)(e\mu)$	–	5.0×10^3	2.5×10^5	4.8×10^4	3.5×10^3	2.8×10^3
$D^- \rightarrow K^+ e^- \mu^-$	$(cd)(us)(e\mu)$	–	2.3×10^4	1.1×10^5	1.1×10^5	1.3×10^4	1.3×10^4
	$(us)(cd)(e\mu)$	–	2.2×10^4	1.1×10^5	1.1×10^5	1.2×10^4	1.2×10^4
$D_s^- \rightarrow \pi^+ e^- \mu^-$	$(cs)(ud)(e\mu)$	–	1.1×10^4	1.4×10^5	1.4×10^5	6.2×10^3	6.2×10^3
	$(ud)(cs)(e\mu)$	–	1.1×10^4	1.4×10^5	1.4×10^5	6.3×10^3	6.3×10^3
$D_s^- \rightarrow K^+ e^- \mu^-$	$(cs)(us)(e\mu)$	–	8.8×10^3	4.4×10^5	7.9×10^4	6.2×10^3	5.0×10^3
	$(us)(cs)(e\mu)$	–	7.9×10^3	3.9×10^5	8.8×10^4	5.6×10^3	4.4×10^3
$B^- \rightarrow \pi^+ e^- \mu^-$	$(ub)(ud)(e\mu)$	–	9.3×10^2	4.0×10^3	4.6×10^4	5.2×10^2	6.6×10^2
	$(ud)(ub)(e\mu)$	–	4.0×10^2	4.9×10^3	2.0×10^4	2.2×10^2	2.8×10^2
$B^- \rightarrow K^+ e^- \mu^-$	$(ub)(us)(e\mu)$	–	9.2×10^2	3.5×10^3	4.6×10^4	5.2×10^2	6.5×10^2
	$(us)(ub)(e\mu)$	–	3.5×10^2	4.4×10^3	1.8×10^4	2.0×10^2	2.5×10^2
$B^- \rightarrow D^+ e^- \mu^-$	$(ub)(cd)(e\mu)$	–	3.2×10^3	4.0×10^4	4.0×10^4	1.8×10^3	1.8×10^3
	$(cd)(ub)(e\mu)$	–	1.3×10^3	1.7×10^4	1.7×10^4	7.5×10^2	7.5×10^2
	$(ud)(cb)(e\mu)$	–	–	3.2×10^4	1.3×10^4	8.9×10^3	3.7×10^3
	$(cb)(ud)(e\mu)$	–	–	1.3×10^4	3.2×10^4	3.7×10^3	8.9×10^3

Table 5: Upper bounds on the Wilson coefficients $C_{4(ijkl)}^{XYZ(\ell_1\ell_2)}$ and $C_{5(ijkl)}^{XYZ(\ell_1\ell_2)}$ extracted from the experimental limits on the LNV meson decays $M_1 \rightarrow M_2 \ell_1^- \ell_2^-$ shown in Table (1), with and without QCD corrections. The bounds in gray background are new results present only after including the effects of QCD corrections, which is the case for all the bounds on $C_{4(ijkl)}^{XYZ(\ell_1\ell_2)}$. Note that the operators bounded by the processes $D^- \rightarrow K^+ \ell_1^- \ell_2^-$ and $D_s^- \rightarrow \pi^+ \ell_1^- \ell_2^-$ mix under RG evolution, so these processes put bounds on the same sets of operators. The operators in light-gray background are improved due to this mixing.

Process	$(ij)(kl)(\ell_1\ell_2)$	Tree Level		With QCD Corrections			
		$C_{6(ijkl)}^{XYZ}$	$C_{6(ijkl)}^{XXX}$	$C_{6(ijkl)}^{LLR,RRL}$	$C_{6(ijkl)}^{LRL,RLR}$	$C_{6(ijkl)}^{LRR,RLL}$	
$K^- \rightarrow \pi^+ e^- \mu^-$	$(us)(ud)(e\mu)$	2.6×10^2	2.8×10^2	2.1×10^2	2.7×10^2	2.7×10^2	
$D^- \rightarrow \pi^+ e^- \mu^-$	$(cd)(ud)(e\mu)$	2.3×10^4	1.9×10^4	2.5×10^4	2.4×10^4	2.4×10^4	
$D^- \rightarrow K^+ e^- \mu^-$	$(cd)(us)(e\mu)$	1.2×10^5	1.1×10^5	1.1×10^5	1.2×10^5	1.2×10^5	
$D_s^- \rightarrow \pi^+ e^- \mu^-$	$(cs)(ud)(e\mu)$	5.1×10^4	4.7×10^4	4.7×10^4	5.3×10^4	5.3×10^4	
$D_s^- \rightarrow K^+ e^- \mu^-$	$(cs)(us)(e\mu)$	4.1×10^4	3.4×10^4	4.5×10^4	4.4×10^4	4.4×10^4	
$B^- \rightarrow \pi^+ e^- \mu^-$	$(ub)(ud)(e\mu)$	1.6×10^3	1.7×10^3	1.3×10^3	1.7×10^3	1.7×10^3	
$B^- \rightarrow K^+ e^- \mu^-$	$(ub)(us)(e\mu)$	1.4×10^3	1.6×10^3	1.2×10^3	1.5×10^3	1.5×10^3	
$B^- \rightarrow D^+ e^- \mu^-$	$(ub)(cd)(e\mu)$	7.0×10^3	6.5×10^3	6.5×10^3	7.4×10^3	7.4×10^3	
	$(ud)(cb)(e\mu)$	—	3.7×10^4	3.7×10^4	—	—	

Table 6: Upper bounds on the Wilson coefficient $C_{6(ijkl)}^{XYZ(e\mu)}$ extracted from the experimental limits on the LNV meson decays $M_1^- \rightarrow M_2^- e^- \mu^-$ shown in Table (1), with and without QCD corrections. The constrained operators involve different lepton flavors ($\ell_1 \neq \ell_2$) since the operator $\mathcal{O}_{6(ijkl)}^{XYZ(\ell_1\ell_2)}$ vanishes otherwise. The bounds in gray background are new results present only after including the effects of QCD corrections. Note that the operators bounded by the processes $D^- \rightarrow K^+ \ell_1^- \ell_2^-$ and $D_s^- \rightarrow \pi^+ \ell_1^- \ell_2^-$ mix under RG evolution, so these processes put bounds on the same sets of operators. The limits for $C_{6(ijkl)}^{LRL,RLR}$ and $C_{6(ijkl)}^{LRR,RLL}$ are the same due to the relation $\mathcal{O}_{6(ijkl)}^{LRZ} = -\mathcal{O}_{6(klij)}^{RLZ}$.

Process	$(ij)(kl)(\ell_1\ell_2)$	Tree Level		With QCD Corrections	
		$C_{7(ijkl)}^{XZZ}$		$C_{7(ijkl)}^{LRR,RLL}$	
$K^- \rightarrow \pi^+ e^- \mu^-$	$(us)(ud)(e\mu)$	–		3.2×10^3	
	$(ud)(us)(e\mu)$	–		3.2×10^3	
$D^- \rightarrow \pi^+ e^- \mu^-$	$(cd)(ud)(e\mu)$	–		2.9×10^5	
	$(ud)(cd)(e\mu)$	–		2.9×10^5	
$D^- \rightarrow K^+ e^- \mu^-$	$(cs)(ud)(e\mu)$	–		1.5×10^6	
	$(ud)(cs)(e\mu)$	–		1.5×10^6	
$D_s^- \rightarrow \pi^+ e^- \mu^-$	$(cd)(us)(e\mu)$	–		6.3×10^5	
	$(us)(cd)(e\mu)$	–		6.3×10^5	
$D_s^- \rightarrow K^+ e^- \mu^-$	$(cs)(us)(e\mu)$	–		5.2×10^5	
	$(us)(cs)(e\mu)$	–		5.2×10^5	
$B^- \rightarrow \pi^+ e^- \mu^-$	$(ub)(ud)(e\mu)$	–		2.0×10^4	
	$(ud)(ub)(e\mu)$	–		2.0×10^4	
$B^- \rightarrow K^+ e^- \mu^-$	$(ub)(us)(e\mu)$	–		1.8×10^4	
	$(us)(ub)(e\mu)$	–		1.8×10^4	
$B^- \rightarrow D^+ e^- \mu^-$	$(cb)(ud)(e\mu)$	–		8.8×10^4	
	$(ud)(cb)(e\mu)$	–		8.8×10^4	

Table 7: Upper bounds on the Wilson coefficient $C_{7(ijkl)}^{XZZ(e\mu)}$ extracted from the experimental limits on the LNV meson decays $M_1^- \rightarrow M_2^- e^- \mu^-$ shown in Table (1), with and without QCD corrections. All the bounds shown in this table (in gray) are new results present only after including the effects of QCD corrections. The constrained operators involve different lepton flavors ($\ell_1 \neq \ell_2$) since the operator $\mathcal{O}_{7(ijkl)}^{XZZ(\ell_1\ell_2)}$ vanishes otherwise. Note that these bounds come from the mixing with the operator $\mathcal{O}_{6(ijkl)}^{XYZ(e\mu)}$, which is constrained at the tree level [see Table (6)]. In particular, the second bound shown for each process is due to the relation $\mathcal{O}_{6(ijkl)}^{RLR,LRL} = -\mathcal{O}_{6(klij)}^{LRR,RLL}$ and the mixing between $\mathcal{O}_{6(ijkl)}^{LRR,RLL}$ and $\mathcal{O}_{7(ijkl)}^{LRR,RLL}$ [see appendix A].

Process	$(ij)(kl)(\ell_1\ell_2)$	Tree Level		With QCD Corrections		
		$C_{1(ijkl)}^{XYZ}$	$C_{2(ijkl)}^{XXX}$	$C_{1(ijkl)}^{XXZ}$	$C_{1(ijkl)}^{(LR,RL)Z}$	$C_{2(ijkl)}^{XXX}$
$\tau^- \rightarrow e^+ \pi^- \pi^-$	$(ud)(ud)(e\tau)$	2.9×10^3	–	1.5×10^3	9.5×10^2	2.9×10^5
$\tau^- \rightarrow e^+ \pi^- K^-$	$(ud)(us)(e\tau)$	3.3×10^3	–	1.7×10^3	1.1×10^3	3.3×10^5
$\tau^- \rightarrow e^+ K^- K^-$	$(us)(us)(e\tau)$	7.1×10^3	–	3.6×10^3	2.3×10^3	7.1×10^5
$\tau^- \rightarrow \mu^+ \pi^- \pi^-$	$(ud)(ud)(\mu\tau)$	4.0×10^3	–	2.0×10^3	1.3×10^3	4.0×10^5
$\tau^- \rightarrow \mu^+ \pi^- K^-$	$(ud)(us)(\mu\tau)$	4.1×10^3	–	2.1×10^3	1.4×10^3	4.1×10^5
$\tau^- \rightarrow \mu^+ K^- K^-$	$(us)(us)(\mu\tau)$	8.6×10^3	–	4.3×10^3	2.8×10^3	8.6×10^5

Table 8: Upper bounds on the Wilson coefficients $C_{1(ijkl)}^{XYZ(\ell\tau)}$ and $C_{2(ijkl)}^{XXX(\ell\tau)}$ extracted from the experimental limits on the LNV tau decays $\tau^- \rightarrow \ell^+ M_1^- M_2^-$ shown in Table (2), with and without QCD corrections. The bounds in gray background are new results present only after including the effects of QCD corrections. The bounds which improve by at least a factor of 2 with respect to the corresponding tree-level bound are shown in light-gray.

Process	$(ij)(kl)(\ell_1\ell_2)$	Tree Level	With QCD Corrections	
		$C_{3(ijkl)}^{XYZ}$	$C_{3(ijkl)}^{XXZ}$	$C_{3(ijkl)}^{(LR,RL)Z}$
$\tau^- \rightarrow e^+\pi^-\pi^-$	$(ud)(ud)(e\tau)$	4.5×10^4	5.9×10^4	5.2×10^4
$\tau^- \rightarrow e^+\pi^-K^-$	$(ud)(us)(e\tau)$	4.4×10^4	5.8×10^4	5.1×10^4
$\tau^- \rightarrow e^+K^-K^-$	$(us)(us)(e\tau)$	7.4×10^4	9.8×10^4	8.5×10^4
$\tau^- \rightarrow \mu^+\pi^-\pi^-$	$(ud)(ud)(\mu\tau)$	6.4×10^4	8.5×10^4	7.4×10^4
$\tau^- \rightarrow \mu^+\pi^-K^-$	$(ud)(us)(\mu\tau)$	5.6×10^4	7.3×10^4	6.4×10^4
$\tau^- \rightarrow \mu^+K^-K^-$	$(us)(us)(\mu\tau)$	9.3×10^4	1.2×10^5	1.1×10^5

Table 9: Upper bounds on the Wilson coefficient $C_{3(ijkl)}^{XYZ(\ell\tau)}$ extracted from the experimental limits on the LNV tau decays $\tau^- \rightarrow \ell^+ M_1^- M_2^-$ shown in Table (2), with and without QCD corrections. For these operators, existing tree-level bounds are not improved by QCD effects.

Process	$(ij)(kl)(\ell_1\ell_2)$	Tree Level		With QCD Corrections			
		$C_{4(ijkl)}^{XYZ}$	$C_{5(ijkl)}^{XYZ}$	$C_{4(ijkl)}^{XXZ}$	$C_{4(ijkl)}^{(LR,RL)Z}$	$C_{5(ijkl)}^{XXZ}$	$C_{5(ijkl)}^{(LR,RL)Z}$
$\tau^- \rightarrow e^+\pi^-\pi^-$	$(ud)(ud)(e\tau)$	–	7.7×10^3	2.6×10^5	7.7×10^5	6.1×10^3	4.9×10^3
$\tau^- \rightarrow e^+\pi^-K^-$	$(ud)(us)(e\tau)$	–	7.0×10^3	7.8×10^4	3.5×10^5	4.0×10^3	5.0×10^3
$\tau^- \rightarrow e^+K^-K^-$	$(us)(us)(e\tau)$	–	7.8×10^3	7.0×10^4	3.9×10^5	4.4×10^3	5.6×10^3
$\tau^- \rightarrow \mu^+\pi^-\pi^-$	$(ud)(ud)(\mu\tau)$	–	1.1×10^4	6.0×10^5	1.8×10^6	1.4×10^4	1.1×10^4
$\tau^- \rightarrow \mu^+\pi^-K^-$	$(ud)(us)(\mu\tau)$	–	8.7×10^3	3.6×10^5	1.1×10^6	8.6×10^3	6.9×10^3
$\tau^- \rightarrow \mu^+K^-K^-$	$(us)(us)(\mu\tau)$	–	9.8×10^3	9.8×10^4	4.4×10^5	4.9×10^3	6.2×10^3
$\tau^- \rightarrow \mu^+K^-K^-$	$(us)(us)(\mu\tau)$	–	2.2×10^4	8.7×10^4	4.9×10^5	5.5×10^3	6.9×10^3
$\tau^- \rightarrow \mu^+K^-K^-$	$(us)(us)(\mu\tau)$	–	2.2×10^4	7.4×10^5	2.2×10^6	1.8×10^4	1.4×10^4

Table 10: Upper bounds on the Wilson coefficients $C_{4(ijkl)}^{XYZ(\ell\tau)}$ and $C_{5(ijkl)}^{XYZ(\ell\tau)}$ extracted from the experimental limits on the LNV tau decays $\tau^- \rightarrow \ell^+ M_1^- M_2^-$ shown in Table (2), with and without QCD corrections. The bounds in gray background are new results present only after including the effects of QCD corrections, which is the case for all the bounds on $C_{4(ijkl)}^{XYZ(\ell\tau)}$.

Process	$(ij)(kl)(\ell_1\ell_2)$	Tree Level		With QCD Corrections			
		$C_{6(ijkl)}^{XYZ}$	$C_{6(ijkl)}^{XXX}$	$C_{6(ijkl)}^{LLR,RRL}$	$C_{6(ijkl)}^{LRL,RLR}$	$C_{6(ijkl)}^{LRR,RLL}$	
$\tau^- \rightarrow e^+\pi^-\pi^-$	$(ud)(ud)(e\tau)$	1.3×10^4	–	–	1.4×10^4	1.4×10^4	
$\tau^- \rightarrow e^+\pi^-K^-$	$(ud)(us)(e\tau)$	1.5×10^4	1.6×10^4	1.2×10^4	1.6×10^4	1.6×10^4	
$\tau^- \rightarrow e^+K^-K^-$	$(us)(us)(e\tau)$	2.8×10^4	–	–	2.9×10^4	2.9×10^4	
$\tau^- \rightarrow \mu^+\pi^-\pi^-$	$(ud)(ud)(\mu\tau)$	1.9×10^4	–	–	2.0×10^4	2.0×10^4	
$\tau^- \rightarrow \mu^+\pi^-K^-$	$(ud)(us)(\mu\tau)$	1.9×10^4	2.1×10^4	1.6×10^4	2.0×10^4	2.0×10^4	
$\tau^- \rightarrow \mu^+K^-K^-$	$(us)(us)(\mu\tau)$	3.5×10^4	–	–	3.7×10^4	3.7×10^4	

Table 11: Upper bounds on the Wilson coefficient $C_{6(ijkl)}^{XYZ(\ell\tau)}$ extracted from the experimental limits on the LNV tau decays $\tau^- \rightarrow \ell^+ M_1^- M_2^-$ shown in Table (2), with and without QCD corrections. The operators not showing a bound vanish due to their symmetry. (One can check that $\mathcal{O}_{6(ijkl)}^{XYZ} = 0$ for $X = Y$, $i = k$, and $j = l$.)

Process	$(ij)(kl)(\ell_1\ell_2)$	Tree Level		With QCD Corrections	
		$C_{7(ijkl)}^{XZZ}$	$C_{7(ijkl)}^{LRR,RLL}$		
$\tau^- \rightarrow e^+\pi^-\pi^-$	$(ud)(ud)(e\tau)$	–	1.7×10^5		
$\tau^- \rightarrow e^+\pi^-K^-$	$(ud)(us)(e\tau)$	–	1.9×10^5		
$\tau^- \rightarrow e^+K^-K^-$	$(us)(us)(e\tau)$	–	1.9×10^5		
$\tau^- \rightarrow \mu^+\pi^-\pi^-$	$(ud)(ud)(\mu\tau)$	–	3.5×10^5		
$\tau^- \rightarrow \mu^+\pi^-K^-$	$(ud)(us)(\mu\tau)$	–	2.4×10^5		
$\tau^- \rightarrow \mu^+K^-K^-$	$(us)(us)(\mu\tau)$	–	2.4×10^5		
$\tau^- \rightarrow \mu^+K^-K^-$	$(us)(us)(\mu\tau)$	–	4.4×10^5		

Table 12: Upper bounds on the Wilson coefficient $C_{7(ijkl)}^{XZZ(\ell\tau)}$ extracted from the experimental limits on the LNV tau decays $\tau^- \rightarrow \ell^+ M_1^- M_2^-$ shown in Table (2), with and without QCD corrections. All the bounds shown in this table (in gray) are new results present only after including the effects of QCD corrections. Note that these bounds come from mixing with the operator $\mathcal{O}_{6(ijkl)}^{XYZ(\ell\tau)}$, which is constrained at the tree level [see Table (11)].

Acknowledgements

We thank Nestor Quintero for valuable discussions. We acknowledge support from Centro de Física Teórica de Valparaíso (CeFiTeV), project PFE UVA22991/PUENTE, ANID (Chile) FONDECYT Iniciación Grant No. 11230879, and ANID REC Convocatoria Nacional Subvención a Instalación en la Academia Convocatoria Año 2020, PAI77200092.

Appendices

A μ -evolution matrices

In this section we list the evolution matrices $\hat{U}(\mu, \Lambda)$ defined in Eq. (25) and calculated from Eq. (58) with the anomalous dimension matrices obtained in Sec. (3). In the calculation we set $\mu = 1 \text{ GeV}$ and $\Lambda = m_Z$. These evolution matrices are used in Sec. (4) to find the RGE-improved bounds on the Wilson coefficients. We organize them in four groups depending on the quark flavor structure of the Wilson coefficients $\mathcal{O}_{n(ijkl)}$ ($ijkl$ indices): (i) Repeated up-flavor quarks, (ii) Repeated down-flavor quarks, (iii) Repeated up- and down-flavor quarks, (iv) all quark flavors different. Similarly to the notation used for the anomalous dimensions in Sec. (3), we assume in the matrices below that the flavor indices i, j, k, l are different, unless explicitly stated.

A.1 Repeated up-flavor quarks ($i = k = u, c$)

$$\hat{U}_{(12)}^{XXZ}(ijil) = \begin{pmatrix} 1.98 & 0.01 \\ -2.87 & 0.44 \end{pmatrix}, \quad \hat{U}_{(13)}^{(LR/RL)Z}(ijil) = \begin{pmatrix} 3.03 & 0. \\ -1.44 & 0.87 \end{pmatrix}, \quad (60)$$

$$\hat{U}_{(3)}^{XXZ}(ijil) = 0.76, \quad \hat{U}_{(44'55')}^{XXZ}(ijil) = \begin{pmatrix} 0.85 & -0.17 & -0.12i & -0.22i \\ -0.17 & 0.85 & -0.22i & -0.12i \\ 0.08i & -0.10i & 1.77 & -0.36 \\ -0.10i & 0.08i & -0.36 & 1.77 \end{pmatrix}, \quad (61)$$

$$\hat{U}_{(45)}^{(LR/RL)Z}(ijil) = \begin{pmatrix} 0.67 & 0.35i \\ 0.02i & 1.41 \end{pmatrix}, \quad \hat{U}_{(6)}^{XXX}(ijil) = 0.91, \quad (62)$$

$$\hat{U}_{(6)}^{XXY}(ijil) = 1.20, \quad \hat{U}_{(67)}^{LRR/RLL}(ijil) = \begin{pmatrix} 0.95 & 0.08i \\ 0 & 1.45 \end{pmatrix}, \quad (63)$$

$$\hat{U}_{(77'8)}^{XXX}(ijil) = \begin{pmatrix} 1.05 & -0.05 & -0.06i \\ -0.05 & 1.05 & 0.06i \\ 0 & 0 & 0.69 \end{pmatrix}. \quad (64)$$

A.2 Repeated down-flavor quarks ($j = l = d, s, b$)

$$\hat{U}_{(12)}^{XXZ}(ijkj) = \begin{pmatrix} 1.98 & 0.01 \\ -2.87 & 0.44 \end{pmatrix}, \quad \hat{U}_{(13)}^{(LR/RL)Z}(ijkj) = \begin{pmatrix} 3.03 & 0. \\ -1.44 & 0.87 \end{pmatrix}, \quad (65)$$

$$\hat{U}_{(3)}^{XXZ}(ijkj) = 0.76, \quad \hat{U}_{(45)}^{XXZ}(ijkj) = \hat{U}_{(\overline{45})}^{XXZ}(ijkj) = \begin{pmatrix} 0.67 & -0.35i \\ -0.02i & 1.41 \end{pmatrix}, \quad (66)$$

$$\hat{U}_{(4\overline{45}5)}^{(LR/RL)Z}(ijkj) = \begin{pmatrix} 0.85 & -0.17 & 0.12i & 0.22i \\ -0.17 & 0.85 & 0.22i & 0.12i \\ -0.08i & 0.10i & 1.77 & -0.36 \\ 0.10i & -0.08i & -0.36 & 1.77 \end{pmatrix}, \quad (67)$$

$$\hat{U}_{(6)}^{XXX}(ijkj) = 1.20, \quad \hat{U}_{(6)}^{LLR/RLL}(ijkj) = 0.91, \quad (68)$$

$$\hat{U}_{(6\overline{7})}^{LRR/RLL}(ijkj) = \begin{pmatrix} 0.95 & 0.08i \\ 0 & 1.45 \end{pmatrix}, \quad \hat{U}_{(7\overline{7}8)}^{XXX}(ijkj) = \begin{pmatrix} 1.45 & -0.45 & -0.03i \\ -0.45 & 1.45 & 0.03i \\ 0 & 0 & 0.69 \end{pmatrix}. \quad (69)$$

A.3 Repeated up- and down-flavor quarks ($i = k = u, c$ and $j = l = d, s, b$)

$$\hat{U}_{(12)}^{XXZ}(ijij) = \begin{pmatrix} 1.98 & 0.01 \\ -2.87 & 0.44 \end{pmatrix}, \quad \hat{U}_{(13)}^{(LR/RL)Z}(ijij) = \begin{pmatrix} 3.03 & 0. \\ -1.44 & 0.87 \end{pmatrix}, \quad (70)$$

$$\hat{U}_{(3)}^{XXZ}(ijij) = 0.76, \quad \hat{U}_{(45)}^{XXZ}(ijij) = \begin{pmatrix} 0.61 & -0.66i \\ -0.03i & 1.26 \end{pmatrix}, \quad (71)$$

$$\hat{U}_{(45)}^{(LR/RL)Z}(ijij) = \begin{pmatrix} 0.73 & -0.04i \\ 0.01i & 1.57 \end{pmatrix}, \quad \hat{U}_{(67)}^{LRR/RLL}(ijij) = \begin{pmatrix} 0.95 & 0.08i \\ 0 & 1.45 \end{pmatrix}. \quad (72)$$

A.4 All different flavor quarks ($i \neq k, j \neq l$)

$$\hat{U}_{(11'22')}^{XXZ}(ijkl) = \begin{pmatrix} 3.26 & -1.28 & -0.06 & 0.07 \\ -1.28 & 3.26 & 0.07 & -0.06 \\ -0.78 & -2.10 & 0.73 & -0.29 \\ -2.10 & -0.78 & -0.29 & 0.73 \end{pmatrix}, \quad (73)$$

$$\hat{U}_{(13')}^{(LR/RL)Z}(ijkl) = \begin{pmatrix} 3.03 & 0 \\ -1.44 & 0.87 \end{pmatrix}, \quad \hat{U}_{(33')}^{XXZ}(ijkl) = \begin{pmatrix} 1.25 & -0.49 \\ -0.49 & 1.25 \end{pmatrix}, \quad (74)$$

Constant	Value	Constant	Value	Constant	Value
m_u	2.16 MeV	m_π	139.57039 MeV	m_e	0.51099895 MeV
m_d	4.67 MeV	m_K	493.677 MeV	m_μ	105.6583755 MeV
m_s	93.4 MeV	m_D	1.86966 GeV	m_τ	1776.86 MeV
m_c	1.27 GeV	m_{D_s}	1.96835 GeV		
m_b	4.18 GeV	m_B	5.27934 GeV		

Table 13: Values of the masses used in our calculations. Taken from Ref. [62].

$$\hat{U}_{(44'55')}^{XXZ}(ijkl) = \begin{pmatrix} 0.85 & -0.17 & -0.12i & -0.22i \\ -0.17 & 0.85 & -0.22i & -0.12i \\ 0.08i & -0.10i & 1.77 & -0.36 \\ -0.10i & 0.08i & -0.36 & 1.77 \end{pmatrix}, \quad (75)$$

$$\hat{U}_{(44'55')}^{(LR/RL)Z}(ijkl) = \begin{pmatrix} 0.85 & -0.17 & 0.12i & 0.22i \\ -0.17 & 0.85 & 0.22i & 0.12i \\ -0.08i & 0.10i & 1.77 & -0.36 \\ 0.10i & -0.08i & -0.36 & 1.77 \end{pmatrix}, \quad (76)$$

$$\hat{U}_{(66')}^{XXX}(ijkl) = \begin{pmatrix} 1.08 & 0.19 \\ 0.19 & 1.08 \end{pmatrix}, \quad \hat{U}_{(66')}^{XXZ}(ijkl) = \begin{pmatrix} 1.08 & -0.19 \\ -0.19 & 1.08 \end{pmatrix}, \quad (77)$$

$$\hat{U}_{(67')}^{LRR/RL}(ijkl) = \begin{pmatrix} 0.95 & 0.08i \\ 0 & 1.45 \end{pmatrix}, \quad (78)$$

$$\hat{U}_{(77'88')}^{XXX}(ijkl) = \begin{pmatrix} 1.44 & 0.02 & -0.07 & -0.39 & -0.05i & 0.01i \\ 0.02 & 1.44 & -0.39 & -0.07 & 0.01i & -0.05i \\ -0.07 & -0.39 & 1.44 & 0.02 & 0.05i & -0.01i \\ -0.39 & -0.07 & 0.02 & 1.44 & -0.01i & 0.05i \\ 0 & 0 & 0 & 0 & 0.69 & 0 \\ 0 & 0 & 0 & 0 & 0 & 0.69 \end{pmatrix}. \quad (79)$$

B Numerical Constants

For the numerical calculations, we use the constants shown in Tables (13) and (14).

References

- [1] J. Schechter and J. W. F. Valle. Neutrinoless Double beta Decay in SU(2) x U(1) Theories. Phys. Rev. D, 25:2951, 1982.
- [2] Werner Rodejohann. Neutrino-less Double Beta Decay and Particle Physics. Int. J. Mod. Phys. E, 20:1833–1930, 2011.

Constant	Value	Constant	Value
τ_K	$1.238 \times 10^{-8} \text{ s}$	f_π	130.2 MeV
τ_D	$1.033 \times 10^{-12} \text{ s}$	f_K	155.7 MeV
τ_{D_s}	$5.04 \times 10^{-13} \text{ s}$	f_D	212 MeV
τ_B	$2.903 \times 10^{-13} \text{ s}$	f_B	190 MeV
τ_τ	$2.903 \times 10^{-13} \text{ s}$		

Table 14: Lifetimes and meson decay constants used in our numerical calculations. Taken from Ref. [62].

- [3] Frank F. Deppisch, Martin Hirsch, and Heinrich Pas. Neutrinoless Double Beta Decay and Physics Beyond the Standard Model. J. Phys. G, 39:124007, 2012.
- [4] S. Abe et al. Search for the Majorana Nature of Neutrinos in the Inverted Mass Ordering Region with KamLAND-Zen. Phys. Rev. Lett., 130(5):051801, 2023.
- [5] Eduardo Cortina Gil et al. Searches for lepton number violating $K^+ \rightarrow \pi^-(\pi^0)e^+e^+$ decays. Phys. Lett. B, 830:137172, 2022.
- [6] Eduardo Cortina Gil et al. Searches for lepton number violating K^+ decays. Phys. Lett. B, 797:134794, 2019.
- [7] Eduardo Cortina Gil et al. Search for Lepton Number and Flavor Violation in K^+ and π^0 Decays. Phys. Rev. Lett., 127(13):131802, 2021.
- [8] Roel Aaij et al. Searches for 25 rare and forbidden decays of D^+ and D_s^+ mesons. JHEP, 06:044, 2021.
- [9] J. P. Lees et al. Searches for Rare or Forbidden Semileptonic Charm Decays. Phys. Rev. D, 84:072006, 2011.
- [10] J. P. Lees et al. Search for lepton-number violating processes in $B^+ \rightarrow h^-l^+l^+$ decays. Phys. Rev. D, 85:071103, 2012.
- [11] Roel Aaij et al. Search for Majorana neutrinos in $B^- \rightarrow \pi^+\mu^-\mu^-$ decays. Phys. Rev. Lett., 112(13):131802, 2014.
- [12] J. P. Lees et al. Search for lepton-number violating $B^+ \rightarrow X-\ell+l^+$ decays. Phys. Rev. D, 89(1):011102, 2014.
- [13] R. Aaij et al. Search for the lepton number violating decays $B^+ \rightarrow \pi^-\mu^+\mu^+$ and $B^+ \rightarrow K^-\mu^+\mu^+$. Phys. Rev. Lett., 108:101601, 2012.
- [14] O. Seon et al. Search for Lepton-number-violating $B^+ \rightarrow D^-l^+l^+$ Decays. Phys. Rev. D, 84:071106, 2011.
- [15] R. Aaij et al. Searches for Majorana neutrinos in B^- decays. Phys. Rev. D, 85:112004, 2012.

- [16] Laurence S. Littenberg and Robert E. Shrock. Upper bounds on lepton number violating meson decays. Phys. Rev. Lett., 68:443–446, 1992.
- [17] N. Quintero, G. Lopez Castro, and D. Delepine. Lepton number violation in top quark and neutral B meson decays. Phys. Rev. D, 84:096011, 2011. [Erratum: Phys.Rev.D 86, 079905 (2012)].
- [18] Hai-Rong Dong, Feng Feng, and Hai-Bo Li. Lepton number violation in D meson decay. Chin. Phys. C, 39(1):013101, 2015.
- [19] Jun-Hao Liu, Jue Zhang, and Shun Zhou. Majorana Neutrino Masses from Neutrinoless Double-Beta Decays and Lepton-Number-Violating Meson Decays. Phys. Lett. B, 760:571–576, 2016.
- [20] Asmaa Abada, Valentina De Romeri, Michele Lucente, Ana M. Teixeira, and Takashi Toma. Effective Majorana mass matrix from tau and pseudoscalar meson lepton number violating decays. JHEP, 02:169, 2018.
- [21] Gorazd Cvetič and C. S. Kim. Sensitivity limits on heavy-light mixing $|U_{\mu N}|^2$ from lepton number violating B meson decays. Phys. Rev. D, 96(3):035025, 2017. [Erratum: Phys.Rev.D 102, 019903 (2020), Erratum: Phys.Rev.D 102, 039902 (2020)].
- [22] Sanjoy Mandal, Manimala Mitra, and Nita Sinha. Constraining the right-handed gauge boson mass from lepton number violating meson decays in a low scale left-right model. Phys. Rev. D, 96(3):035023, 2017.
- [23] Jhovanny Mejia-Guisao, Diego Milanés, Néstor Quintero, and José D. Ruiz-Alvarez. Lepton number violation in B_s meson decays induced by an on-shell Majorana neutrino. Phys. Rev. D, 97(7):075018, 2018.
- [24] Han Yuan, Tianhong Wang, Yue Jiang, Qiang Li, and Guo-Li Wang. Four-body decays of B meson with lepton number violation. J. Phys. G, 45(6):065002, 2018.
- [25] Eung Jin Chun, Arindam Das, Sanjoy Mandal, Manimala Mitra, and Nita Sinha. Sensitivity of Lepton Number Violating Meson Decays in Different Experiments. Phys. Rev. D, 100(9):095022, 2019.
- [26] Rohini M. Godbole, Siddharth P. Maharathy, Sanjoy Mandal, Manimala Mitra, and Nita Sinha. Interference effect in lepton number violating and conserving meson decays for a left-right symmetric model. Phys. Rev. D, 104(9):095009, 2021.
- [27] Frank F. Deppisch, Kåre Fridell, and Julia Harz. Constraining lepton number violating interactions in rare kaon decays. JHEP, 12:186, 2020.
- [28] Y. Miyazaki et al. Search for Lepton-Flavor-Violating and Lepton-Number-Violating $\tau \rightarrow \ell h h'$ Decay Modes. Phys. Lett. B, 719:346–353, 2013.
- [29] Y. Miyazaki et al. Search for Lepton Flavor and Lepton Number Violating tau Decays into a Lepton and Two Charged Mesons. Phys. Lett. B, 682:355–362, 2010.

- [30] A. Ilakovac. Probing lepton number / flavor violation in semileptonic τ decays into two mesons. Phys. Rev. D, 54:5653–5673, 1996.
- [31] Gabriel Lopez Castro and Nestor Quintero. Lepton number violating four-body tau lepton decays. Phys. Rev. D, 85:076006, 2012. [Erratum: Phys.Rev.D 86, 079904 (2012)].
- [32] Han Yuan, Yue Jiang, Tian-hong Wang, Qiang Li, and Guo-Li Wang. Testing the nature of neutrinos from four-body τ decays. J. Phys. G, 44(11):115002, 2017.
- [33] J. Kaulard et al. Improved limit on the branching ratio of $\mu^- \rightarrow e^+$ conversion on titanium. Phys. Lett. B, 422:334–338, 1998.
- [34] F. Simkovic, P. Domin, S. V. Kovalenko, and Amand Faessler. The (muon-, e+) conversion in nuclei mediated by light Majorana neutrinos. Part. Nucl. Lett., 104:40–52, 2001.
- [35] Fedor Simkovic, Amand Faessler, Sergey Kovalenko, and Ivan Schmidt. The (muon-, muon+) conversion in nuclei as a probe of new physics. Phys. Rev. D, 66:033005, 2002.
- [36] Jeffrey M. Berryman, André de Gouvêa, Kevin J. Kelly, and Andrew Kobach. Lepton-number-violating searches for muon to positron conversion. Phys. Rev. D, 95(11):115010, 2017.
- [37] Beomki Yeo, Yoshitaka Kuno, MyeongJae Lee, and Kai Zuber. Future experimental improvement for the search of lepton-number-violating processes in the $e\mu$ sector. Phys. Rev. D, 96(7):075027, 2017.
- [38] B. C. Allanach, C. H. Kom, and H. Pas. LHC and B physics probes of neutrinoless double beta decay in supersymmetry without R-parity. JHEP, 10:026, 2009.
- [39] J. C. Helo, M. Hirsch, H. Päs, and S. G. Kovalenko. Short-range mechanisms of neutrinoless double beta decay at the LHC. Phys. Rev. D, 88:073011, 2013.
- [40] J. C. Helo, M. Hirsch, S. G. Kovalenko, and H. Pas. Neutrinoless double beta decay and lepton number violation at the LHC. Phys. Rev. D, 88(1):011901, 2013.
- [41] Tao Peng, Michael J. Ramsey-Musolf, and Peter Winslow. TeV lepton number violation: From neutrinoless double- β decay to the LHC. Phys. Rev. D, 93(9):093002, 2016.
- [42] L. Gonzalez, J. C. Helo, M. Hirsch, and S. G. Kovalenko. Scalar-mediated double beta decay and LHC. JHEP, 12:130, 2016.
- [43] H. Pas, M. Hirsch, H. V. Klapdor-Kleingrothaus, and S. G. Kovalenko. A Superformula for neutrinoless double beta decay. 2. The Short range part. Phys. Lett. B, 498:35–39, 2001.
- [44] Nestor Quintero. Constraints on lepton number violating short-range interactions from $|\Delta L| = 2$ processes. Phys. Lett. B, 764:60–65, 2017.
- [45] Namit Mahajan. Neutrinoless Double- β Decay and QCD Corrections. Phys. Rev. Lett., 112(3):031804, 2014.

- [46] M. González, M. Hirsch, and S. G. Kovalenko. QCD running in neutrinoless double beta decay: Short-range mechanisms. Phys. Rev. D, 93(1):013017, 2016. [Erratum: Phys.Rev.D 97, 099907 (2018)].
- [47] Carolina Arbeláez, Marcela González, Sergey Kovalenko, and Martin Hirsch. QCD-improved limits from neutrinoless double beta decay. Phys. Rev. D, 96(1):015010, 2017.
- [48] Carolina Arbeláez, Marcela González, Martin Hirsch, and Sergey Kovalenko. QCD Corrections and Long-Range Mechanisms of neutrinoless double beta decay. Phys. Rev. D, 94(9):096014, 2016. [Erratum: Phys.Rev.D 97, 099904 (2018)].
- [49] Marcela González, Martin Hirsch, and Sergey Kovalenko. Neutrinoless double beta decay and QCD running at low energy scales. Phys. Rev. D, 97(11):115005, 2018.
- [50] César Ayala, Gorazd Cvetič, and Lorena Gonzalez. Evaluation of neutrinoless double beta decay: QCD running to sub-GeV scales. Phys. Rev. D, 101(9):094003, 2020.
- [51] Andrzej J. Buras. Weak Hamiltonian, CP violation and rare decays. In Les Houches Summer School in Theoretical Physics, Session 68., pages 281–539, 6 1998.
- [52] Yi Liao, Xiao-Dong Ma, and Hao-Lin Wang. Effective field theory approach to lepton number violating decays $K^\pm \rightarrow \pi^\mp l^\pm l^\pm$: short-distance contribution. JHEP, 01:127, 2020.
- [53] Yi Liao, Xiao-Dong Ma, and Hao-Lin Wang. Effective field theory approach to lepton number violating decays $K^\pm \rightarrow \pi^\mp l_\alpha^\pm l_\beta^\pm$: long-distance contribution. JHEP, 03:120, 2020.
- [54] Marcela González, Sergey Kovalenko, Nicolás A. Neill, and Jonatan Vignatti. RGE effects on the LFV scale from meson decays. Eur. Phys. J. C, 82(4):312, 2022.
- [55] Yi Liao, Xiao-Dong Ma, and Hao-Lin Wang. Effective field theory approach to lepton number violating τ decays. Chin. Phys. C, 45(7):073102, 2021.
- [56] Francesco D’Eramo, Bradley J. Kavanagh, and Paolo Panci. You can hide but you have to run: direct detection with vector mediators. JHEP, 08:111, 2016.
- [57] Fady Bishara, Joachim Brod, Benjamin Grinstein, and Jure Zupan. Renormalization Group Effects in Dark Matter Interactions. JHEP, 03:089, 2020.
- [58] M. U. Ashraf et al. High Intensity Kaon Experiments (HIKE) at the CERN SPS Proposal for Phases 1 and 2. 11 2023.
- [59] Florian Bonnet, Martin Hirsch, Toshihiko Ota, and Walter Winter. Systematic decomposition of the neutrinoless double beta decay operator. JHEP, 03:055, 2013. [Erratum: JHEP 04, 090 (2014)].
- [60] Andre de Gouvea and James Jenkins. A Survey of Lepton Number Violation Via Effective Operators. Phys. Rev. D, 77:013008, 2008.

- [61] Gerhard Buchalla, Andrzej J. Buras, and Markus E. Lautenbacher. Weak decays beyond leading logarithms. Rev. Mod. Phys., 68:1125–1144, 1996.
- [62] R. L. Workman and Others. Review of Particle Physics. PTEP, 2022:083C01, 2022 and 2023 update.